UNIVERSIDAD REGIONAL AMAZÓNICA IKIAM

Ciencias de la Vida

Ingeniería en Biotecnología

Synthesis of carbon dots from bamboo (*Guadua angustifolia* Kunth) wood residues and optimization through response surface methodology

Proyecto de investigación previo a la obtención de Título de:

INGENIERO EN BIOTECNOLOGÍA

AUTOR: JORDY DANIEL INFANTE ERAZO

TUTORA: PhD. Yanet Tibaire Villasana Aguilera

COTUTOR: PhD. Carlos Andres Navas Cárdenas

Napo – Ecuador

2023

DECLARACIÓN DE DERECHO DE AUTOR, AUTENTICIDAD Y RESPONSABILIDAD

Yo, Jordy Daniel Infante Erazo con documento de identidad N°1720528262, declaro que los resultados obtenidos en la investigación que presento en este documento final, previo a la obtención del título de Ingeniero en Biotecnología son absolutamente inéditos, originales, auténticos y personales.

En virtud de lo cual, el contenido, criterios, opiniones, resultados, análisis, interpretaciones, conclusiones, recomendaciones y todos los demás aspectos vertidos en la presente investigación son de mi autoría y de mi absoluta responsabilidad.

Por la favorable atención a la presente, suscribo de usted,

Atentamente,

Tena, 20 de septiembre de 2023

Jordy Daniel Infante Erazo
C.I: 1720528262

AUTORIZACIÓN DE PUBLICACIÓN EN EL REPOSITORIO INSTITUCIONAL

Yo, Jordy Daniel Infante Erazo, con documento de identidad N°1720528262, en calidad de autor y titular de los derechos morales y patrimoniales del trabajo de titulación: “Synthesis of carbon dots from bamboo (Guadua angustifolia Kunth) wood residues and optimization through response surface methodology” de conformidad con el Art. 114 del CÓDIGO ORGÁNICO DE LA ECONOMÍA SOCIAL DE LOS CONOCIMIENTOS, CREATIVIDAD E INNOVACIÓN, reconozco a favor de la Universidad Regional Amazónica Ikiam una licencia gratuita, intransferible y no exclusiva para el uso no comercial de la obra, con fines estrictamente académicos.

Así mismo autorizo a la Universidad Regional Amazónica Ikiam para que realice la publicación de este trabajo de titulación en el Repositorio Institucional de conformidad a lo dispuesto en el Art. 144 de la Ley Orgánica de Educación Superior.

Tena, 20 de septiembre de 2023

Jordy Daniel Infante Erazo
1720528262

CERTIFICADO DE DIRECCIÓN DE TRABAJO DE TITULACIÓN

Certifico que el trabajo de titulación: "Synthesis of carbon dots from bamboo (*Guadua angustifolia* Kunth) wood residues and optimization through response surface methodology" en la modalidad de: tesis, fue realizado por Jordy Daniel Infante Erazo, bajo mi dirección.

El mismo ha sido revisado en su totalidad y analizado por la herramienta de verificación de similitud de contenido; por lo tanto, cumple con los requisitos teóricos, científicos, técnicos, metodológicos y legales establecidos por la Universidad Regional Amazónica Ikiam, para su entrega y defensa.

Tena, 20 de septiembre de 2023

PhD. Yanet Tibaire Villasana Aguilera
C.I: 1757250046

PhD. Carlos Andres Navas Cárdenas
C.I: 0502389000

DEDICATORIA

Esta tesis no tiene un gran aporte a la transcendencia del ser humano, pero sí la tiene para mi familia, ya que juntos culminamos este proceso. Toda mi dedicación se destinará para agradecerles, al igual que a la naturaleza por su gran amor.

AGRADECIMIENTOS

Inicialmente quiero agradecer a las personas que me inculcaron una curiosidad innata en el tema de esta investigación, mis profesores Yanet Villasana, Carlos Navas, Miguel Herrera y Miguel Quishpe, debido a que siempre trataron de motivarme y guiarme en los momentos que más he desconfiado del proceso.

Gracias a ellos, al equipo de técnicas de laboratorios de la Universidad Regional Amazónica Ikiam, en especial a Liz Andi por su paciencia y apoyo. Además, al equipo del Dr. Alexis Debut de la Universidad de las Fuerzas Armadas (ESPE) por la paciencia y disposición de colaborarme siempre de una manera amable en el desarrollo de este proyecto.

Por puesto, agradezco mucho a mi familia por el ser la guía y el soporte de mi ser, por lo tanto, también de este proceso, además también agradezco a mis amigxs y conocidxs, por siempre confiar en mí y demostrarlo con sus palabras y actos.

Finalmente agradezco a la naturaleza, este todo universal lo cual todo inspira.

ÍNDICE GENERAL

ÍNDICE DE TABLAS

ÍNDICE DE FIGURAS

RESUMEN

Los puntos de carbono (PC) son nanomateriales sintetizados a partir de diversas fuentes de carbono mediante diferentes métodos. Entre ellos, destaca la síntesis hidrotermal, que es respetuosa con el medio ambiente, tiene rendimientos del 1% y genera productos con diversas aplicaciones. En este artículo, informamos sobre un método para la síntesis de PC a partir de residuos maderables de bambú (RMB), un análisis de la composición de los RMB, un modelo para la optimización de las condiciones de síntesis y la caracterización espectroscópica de los nanomateriales. Para preparar los PC, los RMB se combinaron con agua en un proceso hidrotermal variando las condiciones experimentales (temperatura y tiempo), seguido de una purificación que consistió en ultrasonidos, centrifugación y filtración. Los PC se analizaron mediante caracterización espectroscópica con absorbancia y fluorescencia. Finalmente, se optimizaron los parámetros de síntesis para obtener una mayor fluorescencia utilizando el método de superficie de respuesta (MSR). El análisis de composición mostró que los residuos de bambú presentan propiedades de residuos lignocelulósicos, debido a los índices estudiados, que incluyen componentes como lignina, celulosa o hemicelulosa en grandes cantidades. La síntesis hidrotermal se realizó utilizando agua desionizada, con condiciones de temperatura entre 160°C y 220°C y un tiempo de 256 a 300 minutos. Los PC con la excitación y concentración más altas en el modelo experimental se obtuvieron a una temperatura de 220°C y un tiempo de 270 minutos. Los resultados de fluorescencia indicaron que los PC obtenidos presentan características de nanopartículas fluorescentes con interés tecnológico que pueden ser funcionalizadas en investigaciones futuras, como aplicaciones de biosensores, bioimagen o soporte fotocatalítico.

Palabras clave: Carbonización hidrotermal, MSR, puntos de carbono, síntesis verde**.**

ABSTRACT

Carbon dots (CDs) are nanomaterials synthesized from various carbon sources by different methods. Among them, hydrothermal synthesis stands out, which is environmentally friendly, has yields around 1% and generates products with diverse applications. In this paper we report a method for synthesis of CDs from bamboo wood residues (BWRs), a compositional analysis of the BWRs, a model for the optimization of synthesis conditions and the spectroscopic characterization of the nanomaterials. To prepare the CDs, BWRs was combined with water in a hydrothermal process varying experimental conditions (temperature and residence time), followed by purification consisting of ultrasonication, centrifugation and filtration. CDs were analyzed through spectroscopic characterization with absorbance and fluorescence. Finally, the synthesis parameters were optimized to obtain higher fluorescence using the response surface method. Compositional analysis showed that bamboo woody residues present properties of lignocellulosic residues, due to the indexes studied there are components such as lignin, cellulose or hemicellulose in large quantities. The hydrothermal carbonization used deionized water, and had temperature conditions between 160°C to 220°C and residence time between 256 - 300 min. The CDs with the highest excitation and concentration in the experimental model were obtained at a temperature of 220°C and a time of 270 min. The fluorescence results indicated that the obtained CDs present characteristics of fluorescent nanoparticles with technological interest that can be functionalized in future research as biosensor, bioimaging or photocatalytic support applications.

Keywords: Carbon dots, green synthesis, hydrothermal carbonization, nanomaterials, RSM.

INTRODUCTION

Nanotechnology is experiencing significant growth due to its capacity to drive technological innovation in various fields. The utilization of nanoscale approaches has led to the presence of nanomaterials in a wide range of products, such as electronics, drugs, stain-resistant clothing, solar cells, cosmetics, food additives, pharmaceuticals, and clean technologies. Furthermore, nanotechnology offers solutions that enhance the interaction between humans and ecological systems, thus contributing to sustainable development. Moreover, nanotechnology is developing a lucrative industry, considering that in 2009 the nanomaterials market generated approximately $225 billion in sales, and has been expanding ever since [1].

Nanomaterials ranging from 1 to 100 nm are of great interest as they exhibit unique properties that vary depending on their size and structure, including magnetic, optical, electrical, structural, and chemical properties. Nevertheless, the increased production and utilization of nanomaterials requires comprehensive studies to ensure their environmental and human health implications [2].

The most prominent nanomaterials are classified based on their dimensions and confinement. However, two-dimensional (2D) materials, such as thin films or quantum wells, are confined in one dimension. One-dimensional (1D) materials, such as quantum wires, are confined in two dimensions, i.e. their atoms are confined in two dimensions, whereas zero-dimensional (0D) materials, such as fullerenes, quantum dots or carbon dots, are confined in three dimensions (3D). It should be noted that the classifications of 0D nanomaterials are still not entirely clear. Carbon dots and quantum dots are the most notable in this category. Carbon Dots and Quantum Dots are the most notable in this category. For example, Carbon Dots are fluorescent carbon nanostructures, whereas Quantum Dots are also carbon nanostructures but with a well-studied discrete quantum structure. To be considered a Quantum Dot, more comprehensive studies are required to understand the nature of quantum mechanics involved in the nanomaterial, such as size-dependent absorption and emission spectra, photoluminescent stability, and quantum yield. Graphene Quantum Dots (GQDs) and Carbon Quantum Dots (CQDs) are derived from Carbon Dots [3–8].

Currently, there is a push to standardize the manufacturing of nanoparticles using green synthesis methods, taking into consideration factors such as the availability of raw materials and other conditions. Carbon Dots (CDs) are nanomaterials that have shown significant contribution to progress in green synthesis, as they can be derived from various carbon sources. The synthesis methods for these CDs have been extensively studied due to the interest in developing nanoparticles with high technological impact. Some of the main investigated applications include biosensors, cellular imaging, drug delivery, targeted therapy, medical diagnosis, bioanalytical assays, photocatalysis, photovoltaic devices, and water and soil treatment [9–13].

Nowadays, there is a growing trend towards environmentally friendly synthesis of nanomaterials, and one of the most promising ones in this regard is CDs. CDs possess unique properties, can be synthesized using eco-friendly principles, and have a wide range of applications. CDs are carbon nanostructures that exhibit fluorescence or phosphorescence, with particle sizes smaller than 10 nm. They are known for their low toxicity, high photo stability, strong fluorescence, and diverse functional groups. CDs are typically quasi-spherical carbon nanoparticles composed of both amorphous and crystalline carbon structures [14]. CDs do not exhibit quantum confinement effects; instead, they are considered 0D nanomaterials with 3D confinement, as they display discrete quantized levels and a different density of states compared to bulk materials [7,8]. The properties of CDs depend primarily on the synthesis method and operational conditions, including precursors, reaction time, solvents, temperature, and more [6]. Furthermore, CDs have attracted considerable interest as possible alternatives to conventional semiconductor quantum dots. They offer excellent optical absorptivity, chemical stability, non-toxicity, easy synthesis, high stability, reduced toxic activity, water solubility, and availability for derivatization. Additionally, CDs exhibit tunable physicochemical and optical properties, and a wide variety of carbon sources can be used for their synthesis [5,6,11].

At present, some strategies have been implemented to develop technologies from agricultural residues to promote a political vision that seeks a balance between economic development and the protection of the environment and resources. This is the case of the Circular Economy, which is focused on prioritizing lower energy consumption, low gas emissions and high efficiency when using technology [16,17]. There are many synthesis methods of CD reported, which are divided into two main groups: top-down and bottom-up methods. Top-down methods allows the uses of carbon pure composites

to extract CDs in form of nanoparticles by chemical oxidation or physical cleavage. Bottom-up methods use carbon-base precursors to form CDs through chemical interactions [11,15,18,19].

In addition, there is an interest in using lignocellulosic biomass as wood or plants like resources of CDs due the carbohydrates in its composition [20]. Lignocellulosic biomass wastes are considered a renewable, green, and affordable raw material. These wastes require pretreatment steps to obtain carbon-based products with desired attributes [21]. The conversion of biomass into a resource with potential applications (e.g., production of carbonaceous composites materials as graphite, carbon foam or biochar from wastes) is considered the principle of green synthesis number 7, use of renewable feedstock. Biomass is a renewable raw material with diverse applications, including the creation of carbon-based materials with added value [16,17,20–23].

In Ecuador there are 600,0026 ha of *Guadua angustifolia* Kunth, a bamboo species that is very popular in the region. This plant is used in several industrial sectors such as agro-industrial production, handicrafts and various services, contributing a total of $475 million to the Ecuadorian economy in 2017. In particular, within the construction industry, the use of bamboo contributes around $100 million annually [24]. Construction with bamboo generates bamboo wood residues (BWRs), being considered as lignocellulosic wastes, a kind of residual biomass. BWRs are a potentially raw material because their components resist to degradation and contain lignin, hemicellulose and cellulose, which are considered precursors of carbon-based materials. Nowadays, thermochemical conversion of lignocellulosic biomass includes hydrothermal carbonization, pyrolysis and gasification. Hydrothermal carbonization (HC) is the most widely used method to synthesize CDs [21]. HC is considered as safe, non-toxic and environmentally friendly method to synthesize CDs from raw materials [20]. HC consists in extracting with water (or some solvent in the case of solvothermal) the components of interest.

In this process a variety of reactions occur such as hydrolysis, dehydration and carboxylation, producing gaseous and water-soluble products [25,26]. Hydrothermal synthesis is accompanied by a purification of the obtained extract, which helps to filter the CDs from other possible components by size. This process is crucial because nanomaterials called CD have a particle size of less than 10 nm [12,27].

The use of lignocellulosic wastes as a raw material in the process of synthesizing nanomaterials should be evaluated to enhance green synthesis. Green synthesis is

considered an emerging trend as it plays a key role in policy, regulation, incentives, and industrial initiatives to reinvent the use of materials [17]. Nowadays, green synthesis of CDs focuses on using plants as feedstock because of their availability, different synthesis methods and a large number of precursor molecules [13]. This kind of synthesis models must be accompanied by appropriate optimization techniques. These are usually mathematical models that optimize processes in terms of criteria of interest [28]. The reaction parameters must be optimized to maximize product yield and application-specific performance while minimizing energy and reactant requirements. One of these models are the Response Surface Method (RSM), which is a technique that can relate the interactions between process parameters and responses [29]. There are various models in RSM, but Central Composite Design (CCD) is the most frequently used for identifying optimal parameters and conducting exploratory analysis of a synthesis process [30].

Synthesis conditions, such as carbon feedstock, temperature and residence time, have a significant impact on CD fluorescence, as well as other properties such as functional groups and particle size. Fluorescence is an optical property of interest that increases at high temperatures, while increasing dwell time can decrease fluorescence intensity [27]. However, these factors have limits, as excessively high temperature can degrade CDs, and prolonged synthesis time can lead to decreased fluorescence. Fluorescence is a key property of CDs [16] because it is a great optical parameter that can show the potentiality as biosensor, this property can also be considered to detect CDs.

Therefore, it is necessary to conduct experimental optimization to determine the ideal conditions that maximize fluorescence. Additionally, there are various chemical and physical mechanisms involved in the synthesis process that should also be taken into account, including the concentration of precursors and the solvents used, which also influence the quality and intensity of CDs' fluorescence [18,25,27,31–35].

CDs have gained significant attention due to their distinctive physicochemical properties, nanoscale size and spectroscopic features such as fluorescence, which make them promising materials for various uses including remediation in water treatment [6], identification of cancer cells [36], monitoring biological environments [37], sensing food contaminants [38] or adsorption of heavy metals [29]. This wide range of applications occurs due to the strong chemical interaction that CDs exhibit, as they can bind to specific molecules through their ions. The use of bamboo wood waste as a source of

CDs is a promising approach for the synthesis of sustainable nanomaterials, taking into account the valorization of lignocellulosic waste [17,21], since the study of this raw material can help to understand the reaction mechanism involved in the synthesis, as well as the properties that CDs may possess, such as functional groups or structure. On the other hand, current research studies on the synthesis of nanomaterials from wood waste are limited. And furthermore, there is a market for this class of nanomaterials, either in the semiconductor industry or in molecular biosensor technologies.

This project describes the process of improving the experimental conditions for a sustainable method of CD synthesis from BWR using HC. The method was created using CCD and refined with RSM. Detection of the resulting CDs was carried out using UV light and spectroscopic techniques, such as absorbance, EDS, TEM, SEM, XRD, FTIR and fluorescence using a microplate spectrophotometer. The objective of the optimization with RSM was to find the appropriate operating conditions to maximize the fluorescence in the synthesized CDs, this was measured with a microplate spectrophotometer. Normally the quantum yield of the CDs is optimized but to reduce the use of toxic solvents, fluorescence was taken as an indicator of the technological interest of the nanomaterial. Therefore, this study aims to address this gap by optimizing the experimental conditions for the synthesis of green CDs from BWR. The results of this research will contribute to the development of sustainable and efficient methods to synthesize nanomaterials from lignocellulosic waste, aligning this practice with SDG 9 (Industry, Innovation and Infrastructure) and the principles of Green Chemistry.

MATERIALS AND METHODS

2.1 Sample preparation

BWRs belonging to the species *G. angustifolia* Kunth were supplied by an Ecuadorian bamboo board factory located in Pedro Vicente Maldonado in Ibarra. These residues were heterogeneous mixture of small-sized particles in the form of chips from the bamboo trunk. The initial treatments of the samples and the proximate analyses were conducted in the biomass laboratory of Ikiam Amazon Regional University. Initially, sample preparation was based on the National Renewable Energy Laboratory (NREL) Laboratory Analytical Procedure (LAP) 510-42620 "Sample Preparation for Compositional Analysis". Samples were washed with deionized (DI) water, dried at 45°C for 30 h to constant weight in an oven (Thermo Scientific, Heratherm) and sieved [39]. Samples smaller than 1 cm sieved with 20 mesh (0.841 mm) were used for compositional analysis, and samples according to 80 mesh with a particle size of 0.180 mm were used for CD synthesis. Subsequently, moisture was measured according to LAP 510-42621 “Determination of Total Solids in Biomass and Total Dissolved Solids in Liquid Process Samples” by drying the samples to constant weigh at 105°C in an oven. This formula was used to [40] calculate the percentage of Moisture (M%) in samples and is expressed as the percentage of the total mass of water present (relative to the total mass sample (Ws). was obtained, which is different before Weigh complete (Wc) and Weigh of pan empty (We)
extraction (A) and after extraction (B).

$$M\% = 100 - ((\left(\frac{Wc - We}{Ws}\right) x100)$$

Briefly, ashes were determinated according to LAP 510-42622 “Determination of Ash in Biomass” by calcining the samples at 575°C for 4 h in a muffle (JP Selecta, N-22 L) and drying to constant weigh. The formula used to calculate ashes [41] considers the difference of weigh between crucibles and sample (Wc) and weigh of crucibles (We), so it are the samples burned in relative of the samples in dry (Sd).

$$A\% = \left(\frac{Wc - We}{Sd}\right) x100)$$

Extractives were determinated according to method T204 “Solvent extractives of wood and pulp” of the Technical Association of the Pulp and Paper Industry (TAPPI) by Soxhlet extraction with 150 ml of 95% ethanol (ISO-Lab) for 18 hours. Contaminants such as waxes, lipids and resins were removed from BWRs with this method [42]. The formula used [42] considers that the percentage of extractives (E%) is obtained by the difference between the weight of the extract (We) and the residue without extract (Wb) in relation to the weight of the wood before extraction (Wp).

$$E\% = [(We - Wb)/Wp] \times 100$$

Three repetitions of each of the analyses indicated in this study were carried out and the values of the standard deviation and the coefficient of variation of each table made it possible to determine the degree of dispersion of the results.

2.2 Proximate analysis of Bamboo wood residues (BWRs)

Samples free of extractives were used to characterize the lignocellulosic composition of bamboo (*G. angustifolia* Kunth), through the quantification of the holocellulose, cellulose, lignin, and hemicellulose, for these compositional analyses methods were approved by the American National Standards Institute (ANSI) were employed. In this case, two replicates were performed for each analysis. Holocellulose composition was measured based on The American Society for Testing and Materials (ASTM) D1104-56 “Method of Test for Holocellulose in Wood” protocol reported by Álvarez et al. [44]. It consists of adding 1 g of sodium chlorite (PanReact) and 0.2 ml of glacial acetic acid (Merck) and heating at 75°C for 5 h until the sample is white. It is then filtered and washed with distilled water. Later, the sample was dried in an on oven to constant weigh. Cellulose was determined by proximate analysis from the test proposed by ANSI T212 - om 18 "Solubility of wood and pulp in 1% sodium hydroxide" with modifications such as concentration of sodium hydroxide solution (Merck) and reaction time. Around three baths with 17.5% sodium hydroxide solution, stirring was carried for 30 min and then solution was vacuum-filtered with Whatman 4 filter paper. The filtrate was then washed with distilled water and 10% acetic acid (Merck) solution and vacuum- filtered. Finally, the samples were oven dried at 105 °C to constant weight [43]. The formula used [43] considers that a percentage of cellulose (S) was obtained, which is different before extraction (A) and after extraction (B).

$$S\% = [(A - B)/A] \times 100$$

Hemicellulose content was calculated by the difference between holocellulose and cellulose quantities. Finally, lignin analysis proceeded according to ANSI´s test T222 – om 02 “Acid-insoluble lignin in wood and pulp” consisting in a hydrolysis of 1 g of BWR of lignin using 10 mL of sulfuric acid 72% v/v (Merck)and shaken. Later a second hydrolysis with a solution of 4% v/v of sulfuric acid and left to boil for 4 h. The sample was decanted and filtered. Finally, it was placed in oven at 105°C for 24 h and weighed. The formula [45] that helps calculate the percentage of lignin (L) present in the sample is as follows:

$$L\ \% = (A \times 100)/W$$

This formula considers that the ratio of the weight of lignin (A) to the constant weight of the sample (W) indicates this value.

2.3 Synthesis and purification of CDs from BWRs (*G. angustifolia* Kunth)

The synthesis of CDs was conducted in the biomass laboratories of Ikiam Amazon Regional University, with the exception of the sonication step, which took place in the natural products laboratories within the same university. BWRs (3.0 g) and deionized water (52.5 ml) were added and sealed in a 100 ml steel reactor for 5 h at 160°C, 180°C, and 200°C in triplicate at each temperature for hydrothermal treatment. The mixture was then vacuum-filtered to separate the solid and liquid phases. The solid phase was discarded, while the liquid phase, containing CDs in the form of dispersed nanoparticles, was collected. These extracts underwent ultrasound irradiated using a bath sonicator (Branson Ultrasonicstm, CPX-952-238R) for 30 minutes, followed by centrifugation at 4,700 rpm for 20 minutes using a centrifuge (Thermo scientific, Sorvall ST40R), and filtration through a 0.22 µm filter. After TEM and SEM characterization, 12 batches (CD 1-12) were synthesized, as the feasibility of the synthesis method had already been established, and 12 samples were required for optimization purposes.

2.4 Detecting CDs with UV-Light

To validate the method, it was necessary to perform a detection step before lyophilization. To detect CDs, a 10 ml dilution of liquids from the batches is placed in 25

ml beakers. A dual wavelength ultraviolet light flashlight is then placed perpendicular to the beakers, emitting light at 365 nm and 395 nm. Making sure that the light directly illuminates the beakers, photographs are taken to capture the fluorescence. In addition, a control is performed using distilled water instead of the target sample.

2.5 Experimental design based in CCD

In this study, a response surface methodology was used to determine the reaction condition parameters that allows to obtain the optimal value of fluorescence of CDs. Composite Central Design (CCD), which is considered an exploratory design technique, was used to design the experimental conditions. With the use of R studio software, the experimental design was determined using the following factor variables: A: Hydrothermal synthesis temperature (180-220°C); B: Residence time (270-330 min) and the CDs concentration was used as the dependent variable (Table 1).

Table 1. Experimental design with factorial variables

			Levels		
Factor	Independent variable	Unit	-1	0	1
A	Temperature	°C	180	200	220
B	Residence time	Min	270	300	330

Created by: Infante, Jordy, 2023.

This formula [46] was used to determine the total number of experiments:

$$N = nf + 2k + nc$$

For this purpose, a total of 12 (N) experiments were performed. Nf corresponds to four factorial points, 2k four axial points (k) and four central points (nc) was chosen.

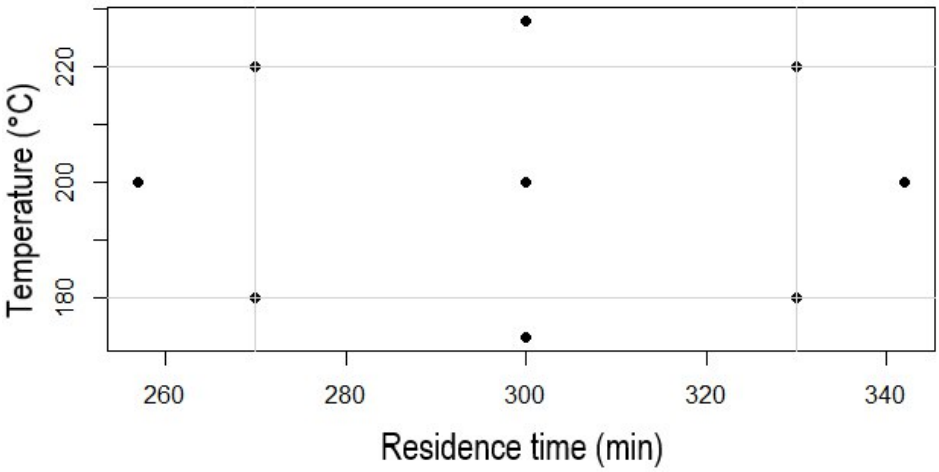

Figure 1. Experimental design based on CCC.
Created by: Infante, Jordy, 2023.

Table 2. Design matrix and fluorescence results

Label	Run	A: Temperature (°C)	B: Residence Time (min)
CD-1	1	180	270
CD-2	2	220	270
CD-3	3	200	257
CD-4	4	173	300
CD-5	5	228	300
CD-6	6	180	330
CD-7	7	220	330
CD-8	8	200	342
CD-9	9	200	300
CD-10	10	200	300
CD-11	11	200	300
CD-12	12	200	300

Created by: Infante, Jordy, 2023.

All solutions, including those synthesized prior to detection, were subjected to vacuum lyophilization with a lyophilizer apparatus (SP Scientific Genevac, BTP-9E LOVE) to obtain lyophilized solid CD samples.

2.6 CDs Characterization

The characterization of the CDs was conducted in different laboratories in Ecuador. Spectroscopic characterizations such as absorbance and fluorescence were carried out in the molecular biology laboratories of Ikiam Amazon Regional University. Initially, a CD

solution with a known concentration ranging from 0 µg/mL to 1 µg/mL was prepared in a 96-well microplate. Subsequently, 200 µL of each CD solution obtained using the CCD experimental design was added to the microplate. Absorbance and fluorescence intensity of each well were then detected using a microplate spectrophotometer (Promega, GloMax Discover System) for the CD solutions obtained after synthesis. With this data, a standard solution was prepared to determine the concentration of CDs based on absorbance, as reported by Chen and their team [37]. Subsequently, a calibration curve of the sample of known concentration was performed using the Lambert-Beer Law [47]. The data were fitted to a linear function to determine the concentrations of the remaining CDs.

After these measurements, dilutions of the CDs of interest were sent to ESPE´s laboratories for TEM, EDS, SEM and XRD analysis and to Yachay Tech´s laboratories for FTIR analysis. Size and morphology of the samples were obtained using a FEI Tecnai G2 spirit twin transmission electron microscope (TEM). The structure and phase purity of the synthesized materials were examined using a Bruker D2 Phaser X-ray diffractometer (XRD), utilizing a copper tube with a wavelength of 1.54184 Å. The diffraction pattern was analyzed using the DIFRACC.EVA V4.3.1.2 software to perform a semi-quantitative analysis and identify any secondary phases. The sample's morphology was investigated through scanning electron microscopy (SEM) and energy-dispersive X-ray spectroscopy (EDS). For this purpose, a field emission electron microscope, specifically the TESCAN MIRA 3 model, equipped with a Bruker X-Flash 6-30 detector with a resolution of 123 eV in Mn Kα was employed. Finally, Fourier Transform Infrared (FTIR) measurements were conducted to characterize the surface functional groups in CDs. The measurements were performed using an Agilent Cary 630 instrument, with a wavelength range of 400-4000 cm^{-1}.

2.7 Response Surface Methodology optimization

The RSM statistical technique optimized the relationship between the independent factors (Residence time and Temperature) with the dependent variable fluorescence through experimental data. The experimental data obtained modeled a second order polynomial equation to determine the effect of the independent variables on the response. The model obtained evaluated the experimental responses based on the following second order polynomial equation:

$$Y = Bo + BiXi + BiiXi2 + BijXiXj + e$$

The quality of the fit was analyzed by the coefficient of determination (R2), the coefficient of variance and the lack of fit [46]. The response surface and contour plots allowed to evaluate the interaction with temperature and time with the fluorescence of the CDs, allowing to find critical points for the optimization of the process.

RESULTS AND DISCUSSION

3.1 Proximate analysis

The main components of *G. angustifolia* Kunth are lignocellulosic as cellulose, hemicellulose, holocellulose and lignin. This analysis has the potential to understand optimal applications based on the compositional characteristics of the raw material. Principal applications can be deriving bioproducts [48], use as raw material, use as fuel for thermal energy generation [49], and other industrial processes focusing in environmental ambit. It´s important to mention that compositional analysis helps to design the synthesis method of the bioproduct. For example, Fahmi *et al.* reports a synthesis method of CDs using as precursor the cellulose present in the leaf of bamboo (*Gigantochloa* apus). These CDs are used for efficient tumor imaging and drug delivery in therapies. Their synthesis design is based on the alkaline hydrolysis of cellulose using NaOH, followed by an additional step of hydrothermal carbonization [50]. There are some reports of CDs made from bamboo, such as that of Liu *et al*. [51], who used washed leaves to synthesize functionalized CDs for use as heavy metal biosensors. Their work focuses on using vitamin C present in bamboo leaves as a carbon source. Another interesting work that performed another biosensor to interact with nitrophenol compounds and this one also uses bamboo leaves [52]. The great advantage of the leaf is that it is easier to manipulate than wood, or wood residues, being affected the properties of the obtained CDs as well as the synthesis conditions.

The results of the composition analysis (Table 3) show similar values to those of Césare *et al.* [53] because the same raw material was used, and results also aligns with the results of Zhang *et al.* [20] who used switchgrass, a lignocellulosic biomass. The composition of biomass may vary when analyzing different bamboo species, each with its own characteristics depending on the species and growth region, which can affect their chemical composition [48]. Among these species, *G. angustifolia* Kunth stands out in Ecuador [24] and is considered a potential resource that can produce high-value products [48]. Sample preparation is critical as the residues used for nanomaterial fabrication often contain impurities. The synthesis method needs to be adapted to the precursor. In this report, the samples were in the form of wood fibers, which are considered shredded construction waste rich in fibers and carbon. To maintain simplicity in the synthesis method, an aqueous extract of polysaccharides was obtained using

BWRs as precursors through a one-pot hydrothermal carbonization process. Wei *et al., r*eports that a biomass is considered lignocellulosic if it has a composition of cellulose between 35% and 50%, hemicellulose between 20% and 35%, and lignin between 10% and 25%. The remaining percentage may vary between proteins, carbohydrates, oils, and ashes. However, despite not meeting the standard for hemicellulose, our samples can still be considered lignocellulosic due to the large amount of holocellulose it contains. The issue with holocellulose is that it is challenging to utilize or degrade [54].

Another key point in the proximal analysis are experimental factors that should always be adapted to the specific biomass being used. In this study, we utilized BWRs and applied analysis protocols for wood and wood pulp, as the samples were in the form of wood chips. For instance, Madan & Pare [55] dried their samples at 80°C in short periods of time showing that bamboo loses moisture by diffusion mechanism, while Césare *et al.* [53] dried their bamboo samples at 105°C for 24 hours, similar to the process employed in this report. Therefore, it makes sense to have obtained similar results in terms of moisture content.

Table 3. Compositional analysis of BWR and comparison with other similar biomasses.

	***G. angustifolia* Kunth**		**Switchgrass**
Component	This study (%)	(Césare *et al*., 2019) (%)	(Zhang, *et al*., 2019)
Moisture	11.11	11.15	-
Ashes	3.20	3.19	4.5
Ethanol extractives	5.82	6.57	5.6
Holocellulose	56.38	54.67	-
Cellulose	48.07	44.49	36.5
Hemicellulose	8.31	10.18	25.4
Lignin	20.2	24.95	19.6

Created by: Infante, Jordy, 2023.

Ashes are considered as mineral and inorganic phase of biomass, but it has components of interest. Lui *et al.* [56], determined that the main components of bamboo (*Pyllocastachys praecox*) ash was K_2O, SiO_2 and SO_3 which can be useful precursors or raw material.

Actually, there are several studies about the applications of *G. angustifolia* Kunth. For example, Marafon *et al.* [49] determined that four bamboo species, including *G angustifolia* Kunth, can be used as fuel for thermal energy at the industrial level due to

lignin and fiber. In addition, the main components of *G. angustifolia* Kunth are pristine CD precursors, cellulose being the most used. Cellulose is one of the most abundant polymers worldwide and contains a quantity of carbon [54]. Therefore, there is much research on how to utilize and functionalize bamboo cellulose and its derivatives. Nanocellulose is also a good raw material for synthesizing CDs, Wei *et al* synthesized nanocellulose hydrogels and CDs with good fluorescent properties [57].

Another study reported the formation of CDs in the grilling process of burgers. Yao and colleagues extracted the carbon from the burgers grilled with ethanol and ethyl acetate, and then performed dialysis to obtain the CDs [58]. Once the proximate composition of the raw material has been accurately determined, it is possible to design or reconsider the synthesis method, taking into account the reaction mechanism. This factor is crucial for developing an effective methodology that allows the capture of carbon-containing molecules, as well as considering the potential for enhancing the properties of CDs through the incorporation of additives or dopant agents. Many carbon-rich materials have been investigated to synthesize CDs, but the key is to identify abundant and renewable raw materials from the environment that can be subjected to a simple and environmentally friendly treatment process to obtain CDs with favorable properties from molecular precursors. Nowadays, there are reviews of lignocellulosic biomass as raw material to obtain CDs and other derivatives [8,21], but Zhang *et al.* [20] focuses in polysaccharides presents in switchgrass to synthesize CDs being an adaptable method. Therefore, the results of the proximal analysis indicate that BWRs can have polysaccharides as precursors for synthesize CDs using the hydrothermal carbonization method.

3.2 Synthesis of CDs from BWR

The Carbon Dots (CDs) synthesis methods based on hydrothermal carbonization (HC) employ deionized water as solvent, due to the simplicity of the process and the absence of complex pretreatment. This method allows the control of time and temperature, as well as the possibility of dividing the extracts obtained into batches for purification. There were two synthesis periods, in the first one the batches of CD-160, CD-180, CD-200, CD-220 were made, and in the other period, the ones designed in CCD (CD 1-12) were made.

Temperature and residence time were considered as factorial conditions due to their importance in the reaction mechanism involved in these phases in order to determine that BWRs can be considered as feedstock of interest for CDs.

Despite that, the reaction mechanism of the reported methodology should resemble the one proposed by Zhang *et al.* [20] and Yahaya *et al.* [29], since in their hydrothermal synthesis mechanism, hydrolysis and carbonization of starch occurs to obtain the CDs. Hydrothermal synthesis is considered the best route to synthesize CDs from biomass [23] and is considered environmentally friendly by using deionized water as solvent. The present method, as well as the reported method, aligns with six principles of Green Chemistry, such as safe synthesis process (3), use of safer chemicals (4), use of safe solvents (5), energy saving (6), use of renewable raw materials (7), and use of safe chemical processes (12). There are other principles as prevent waste (1), atom economy (2), reduce derivatives (8), catalysis (9), design for degradation (10), and real time analysis for pollution prevention (10) [12,17].

To evaluate the physical and chemical transformations that take place during hydrothermal treatment conditions, such as partial decomposition of polysaccharides, reduction of water content, carbonization and CO2 generation, both residues and aqueous extracts should be studied by chemical and physical analysis. This is complemented by experimental results from studies involving mass, atomic, molar, and other types of analyses to gather additional information, as seen in thermogravimetric analysis (TGA) and High-Performance Liquid Chromatography (HPLC). It's worth noting that other studies have explored alternative techniques for lignocellulosic residues. For instance, Zhang *et al.* [20] utilized switchgrass, calculated the carbon content in its biomass, and examined the polysaccharides present in different extracts using techniques like TGA and HPLC.

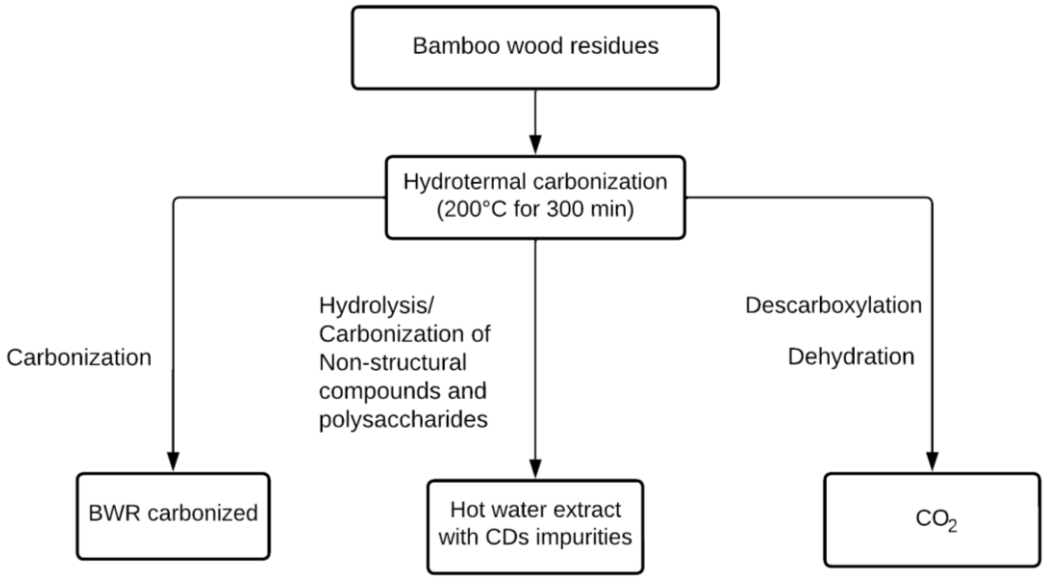

Figure 2. Possible degradation routes in the hydrothermal synthesis of CDs.
Created by: Infante, Jordy, 2023.

Temperature and time are fundamental factors in the degradation of the structural polysaccharides that compose biomass, therefore it is crucial to find the optimal points to have a better performance [18]. In this case, these conditions have been studied in reference to increase the fluorescence values.

The report used as a reference for the first syntheses was Zhang *et al.* [20] which recommends setting as parameters for one-pot synthesis a temperature around 200°C for 5 h focusing on carbonizing the BWRs and extracting the polysaccharides to purify them from the extract obtained. These synthesis trials helped to standardize the purification process. In this first batch process, the synthesized CDs have a mass yield of 4.06 wt% at 200°C for 5 h, i.e., 0.1218 g of CDs were obtained from 3 g of the bamboo mass.

The raw material usually has a variety of compounds but using more purified components provides purer products. The synthesis of CDs from biomass waste is simple, economically favorable and readily available in nature [8], being the case of BWRs. This method is functional to test with other types of biomasses, since there are reports of CD synthesis with many carbon sources. In addition, it should be noted that in hydrothermal carbonization CDs are usually doped with nitrogen using additives such as ammonium bicarbonate or ammonium hydroxide, this doping has provided nanoparticles of interest with additional functional applications and properties [23,59].

3.3 Characterization of CDs using spectroscopic and microscopes techniques

3.3.1 Concentration and absorbance of CDs batches

Initially, the behavior of the absorbance at different wavelengths was checked to calculate the absorbance. To estimate the concentration value, the behavior of the samples at 600 nm excitation of absorbance was used because it was the only measurement filter that behaved entirely linearly, as demonstrated by figure 3. Therefore, the absorbance data at this wavelength was used to calculate the concentrations of the other CD batches using their absorbance value. All batches have different concentrations because they had different synthesis parameters. To calculate the concentration 0.50 g of CD-12 batch powder was used to make a solution with a known concentration. The yield of the batches ranged from 5% to 17% of CDs based on the biomass used.

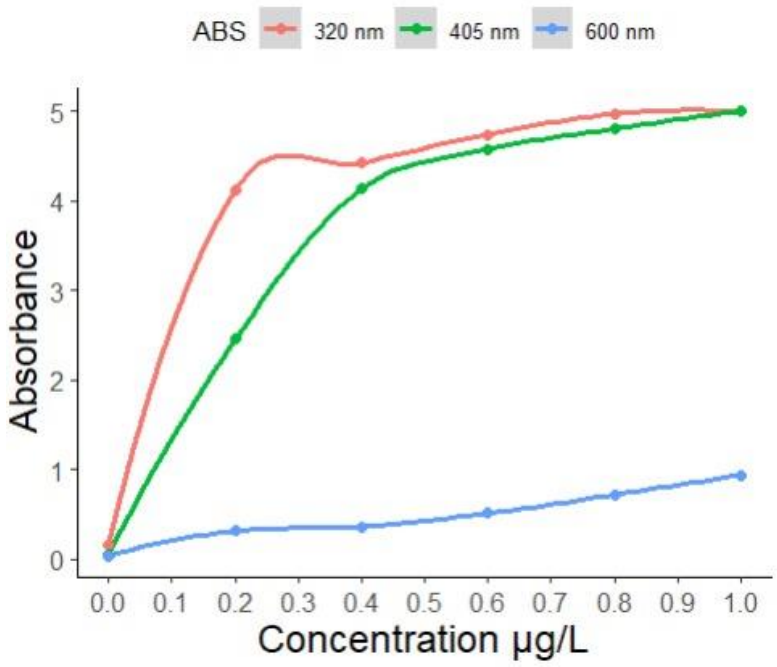

Figure 3. Absorbance at different ranges of a carbon dot of a known concentration.
Created by: Infante, Jordy, 2023.

Figure 3 also shows that the best wavelengths to detect the Carbon Dots are 320 nm and 405 nm of excitation of absorbance, as it becomes saturated. These wavelengths were chosen due to the specificity of the equipment. Literature indicates that the best range to detect CDs with absorbance is 350-650 but normally the excitation wavelength is between 365 nm and 400 nm [60,61]. In addition, Figure 3 shows the lineal range exceed on the concentration in wavelengths 365 nm and 405 nm because samples are

saturated, so dilute samples were a great solution. In this case, linear range is saturated, so absorbance can be inexact.

For this reason, next step was calibrating using the wavelength at 600 nm because it has a lineal range that don´t exceed the value 1 in absorbance, remaining concentration with the obtained linear regression equation through absorbance measurement. The generated linear regression presented a coefficient of determination (R^2) of 0.9729 (fig. 4) so the fit was reliable to calculate the remaining concentrations using Lambert-Beer Law [47].

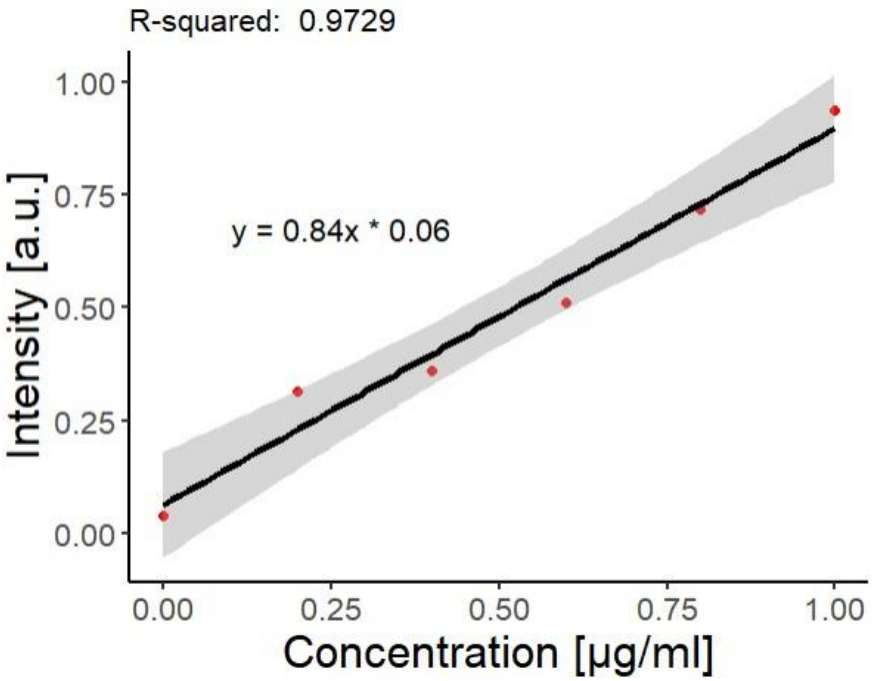

Figure 4. Calibration curve of concentration of batch CD-12 with absorbance taken at 600 nm.
Created by: Infante, Jordy, 2023.

All the CDs were obtained from 3,000 g of feedstock, so the difference in their synthesis conditions lies only in temperature and time. The mass yield of the CDs ranged from 1% to almost 5%. Figure 5 shows the concentration of each CDs batch, showing that CD-2 made at 220°C and 270 min was the most concentrate, this batch was synthesized with a high temperature and lower time.

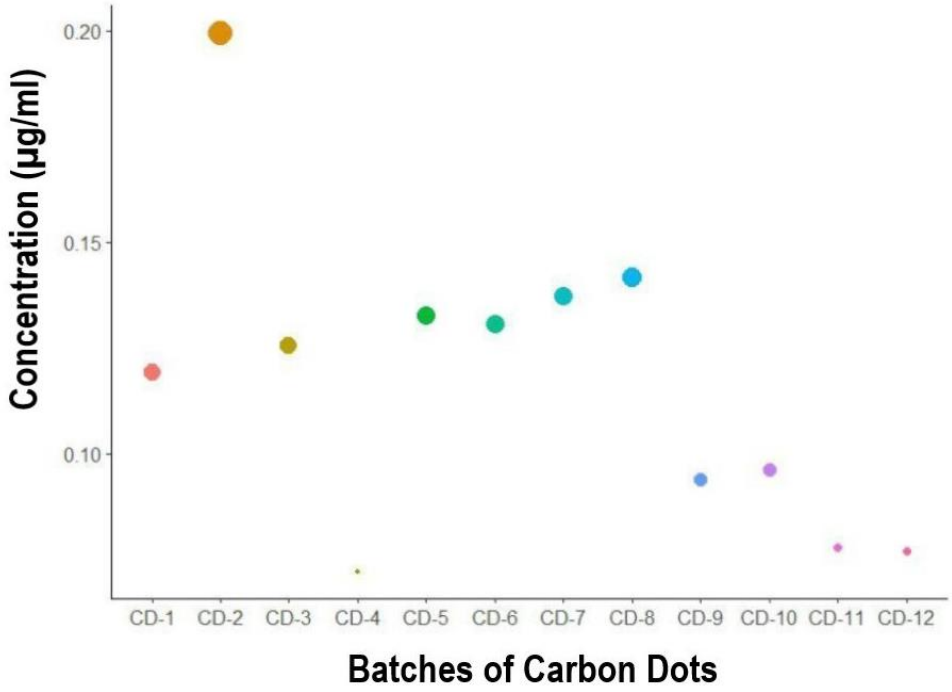

Figure 5. Concentration of CDs obtained in experiments based on absorbance (colors indicate the different batches)
Created by: Infante, Jordy, 2023.

Other experiments with lignocellulosic biomass reported that the best parameters to synthesize CDs was 220°C for 5 h [20], showing that temperature could be the principal factor. For this reason, the initial experiments only change temperature taking time as constant. The high temperature and residence time could have degraded the structural polysaccharides that form the CDs [18], because the batches corresponding to the central points (CD-9-10-11-12) have a high residence time (300 min) and moderate temperature (200°C). Figure 5 also denoted that CD 2 has the major absorbance value. This assay is recommended to be complemented with UV-VIS to check the behavior of the excitation peaks that the CDs may have.

The absorbance values were taken to determine if the obtained CDs can be used as detectors in various applications, such as biosensors, imaging devices, and photodynamic therapy [34,62]. For example, Senthamizhan's team designed hydrochromic CDs as intelligent sensors to detect organic solvents due to the remarkable optical properties exhibited by their CDs, including absorbance values [63]. This value has also been useful in indicating whether CDs can serve as dual-emission radiometric fluorescence sensors for detecting dopamine [64].

Figure 6 reconfirmed that the optimal wavelength to detect CD was 320 nm, since there is a higher absorption. Furthermore, it can be seen that the absorption behavior in the different batches was similar, so it can be stated that the calculated concentration values shown in Figure 5 are well estimated. Therefore, the concentration values in Figure 5 would be the concentration values at which the absorbance and fluorescence data were measured.

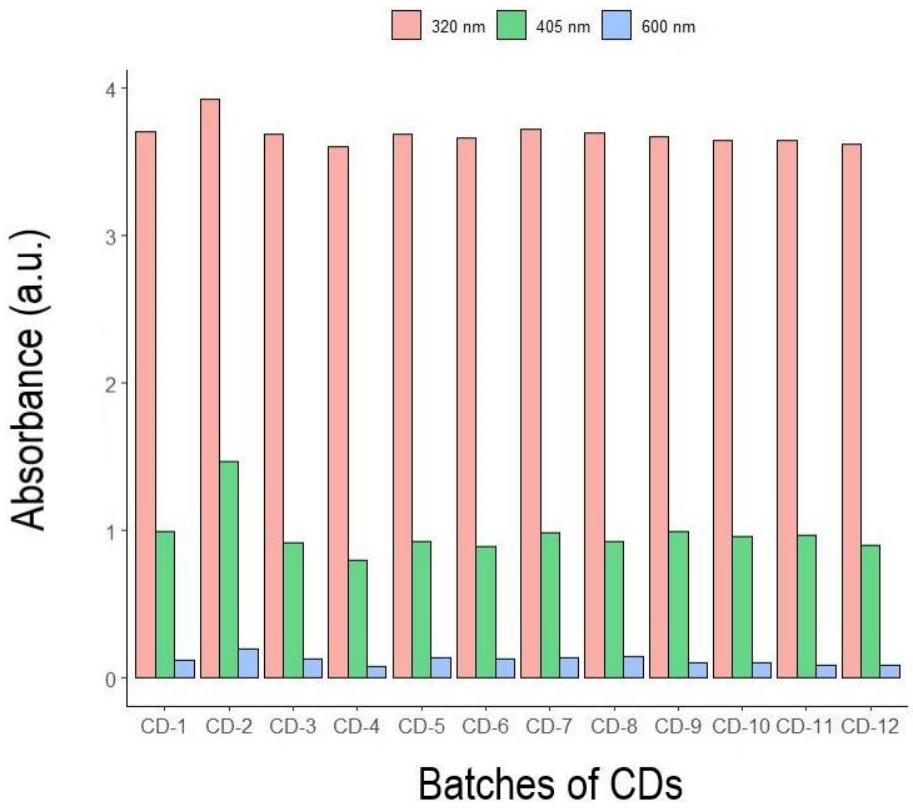

Figure 6. Absorbance at different excitation wavelengths of CDs obtained in experiments.
Created by: Infante, Jordy, 2023.

Both figures (3 and 6) shows the same tendency that the wavelength of 600 nm is the worst wavelength to detect CD as literature confirms because CDs are normally excited under UV light [65]. In other words, absorbance and fluorescence at 320 nm and 405 nm help us detect the CDs, while absorbance at 605 nm assists in calculating the concentration of the batches.

3.3.2 Fluorescence of CDs batch

All CDs solutions obtained showed a great fluorescence intensity without any coupling or dopant agent. The fluorescence value of the solution obtained from batch CD-12 was

also determined at different emission wavelengths, and it was found that a wavelength close to visible light provides the highest fluorescence intensity. Furthermore, the fluorescence behavior at longer wavelengths approaches linearity, confined within a range of concentrations. Figure 7 shows that the best emission wavelength for detecting CDs is in the near UV region, in this case due to the conditions of the apparatus the range was 415 to 445 nm. However, the highest peak fluorescence emission of CDs is usually reported below 405 nm [16,60].

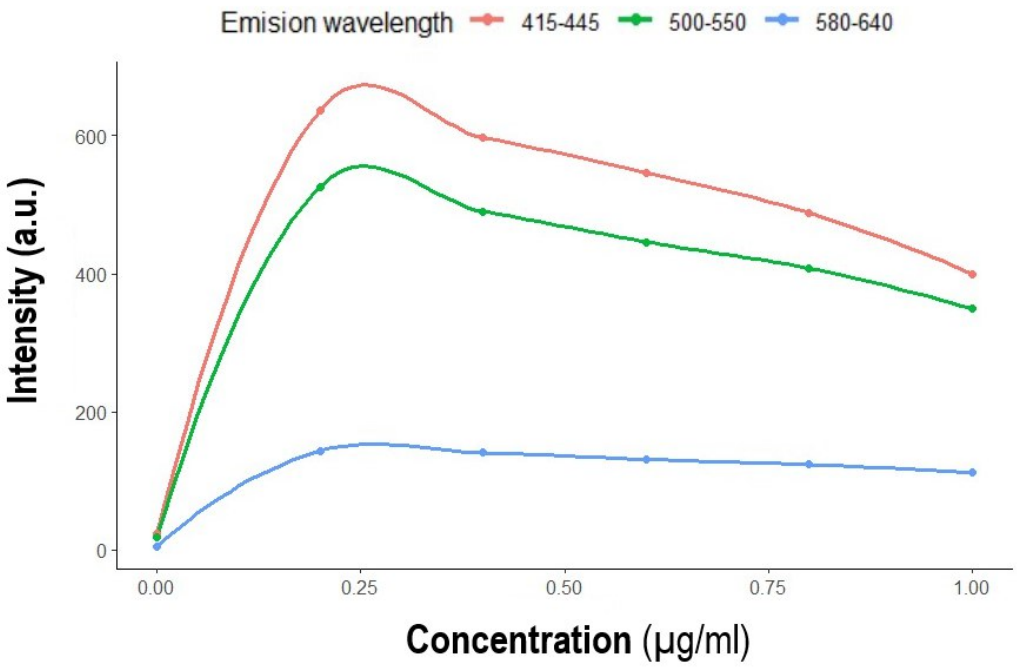

Figure 7. Fluorescence at different ranges of a carbon dots of known concentration
Created by: Infante, Jordy, 2023.

The nanoparticles show bright blue fluorescence under 365 nm ultraviolet light [23]. Figure 8 shows the fluorescence emission under ultraviolet light of different wavelengths. Figure 8a shows a control sample composed of distilled water under 365 nm ultraviolet light. In Figure 8b, corresponding to the 395 nm light the color observed was somewhat greenish and in Figure 8c, the light used was 365 nm in which the light blue reported at this wavelength can be observed. The color obtained in solution resembles the cyan/blue of Perumal *et al.* [60], who synthesized nitrogen-doped CDs from Red Malus floribunda fruit and ammonium hydroxide to remove heavy metal ions.

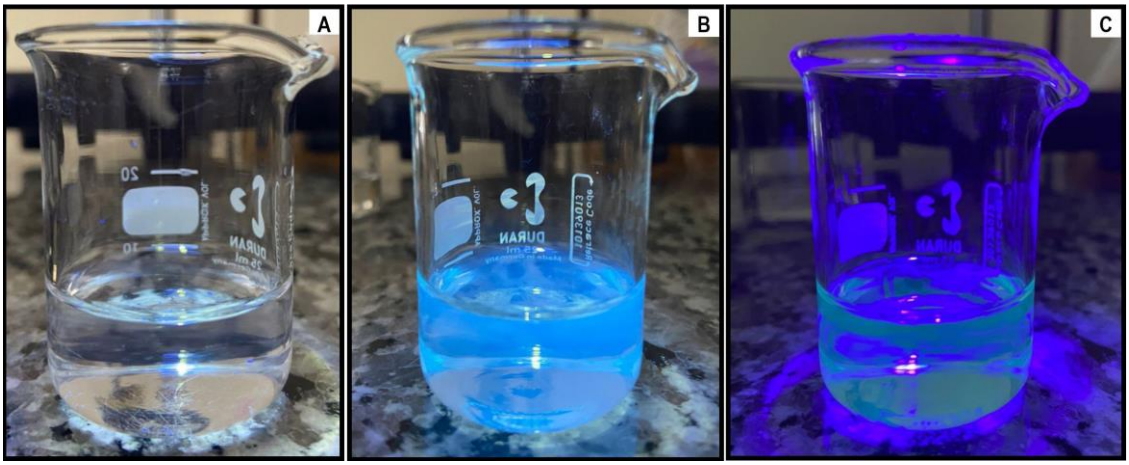

Figure 8. Fluorescence emission of CDs under UV light. A) deionized water as control, b) CD-9 solution under 365 nm UV light, c) CD-9 solution under 395 nm UV Light.
Created by: Infante, Jordy, 2023.

In Figure 9, it can be seen that CD-2 is the treatment that presented the highest fluorescence intensity. In this case, similar to Figure 6, the central spots (CD 9-12) show similar behavior. The high fluorescence intensity on CD-2 also indicates a higher concentration of CDs present. In addition, it can be observed that the nanoparticles in most conditions show an intensity of 500 units, having slight excitation units in the range of 500-550 in most treatments. These measurements can be improved with sensitivity at 365 nm or by doping the CDs [16].

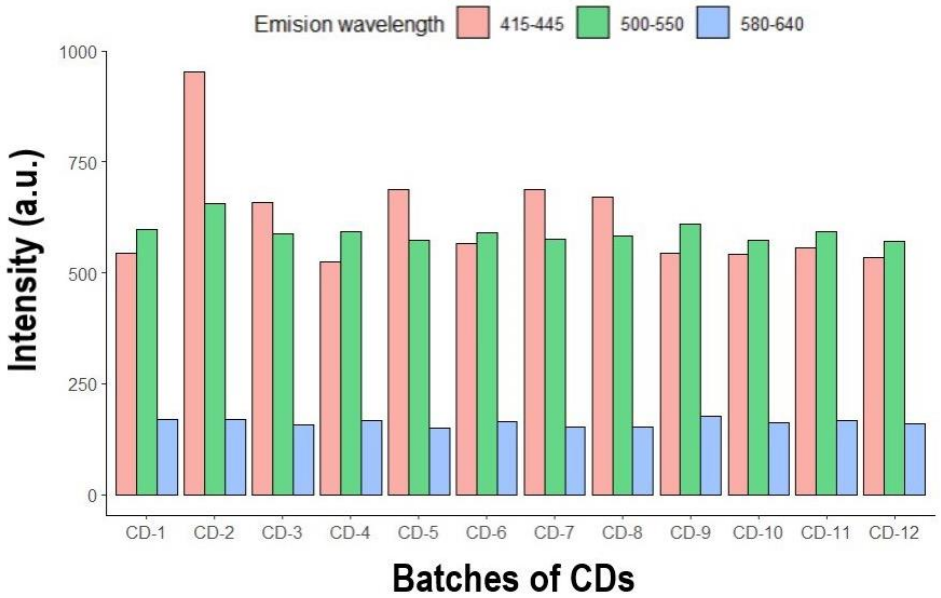

Figure 9. Fluorescence of CDs obtained in experiments.
Created by: Infante, Jordy, 2023.

The batches of CDs exhibit these favorable optical characteristics. However, it is necessary to implement additional characterization techniques that provide more information to ensure its use and quality, indicating others possible potential applications These optical properties indicated that the synthesized nanoparticles have potential applications, especially as biosensors or for bioimaging [23,60,66].

3.4 TEM

The dot size and morphology of the obtained samples was analyzed using Transmission Electron Microscopy (TEM). Initially, two samples were analyzed: CD-180 and B1. CD-180 corresponds to the first synthesis batch, while B1 corresponds to the lyophilized product of the liquid extract from CD-180. The B1 sample exhibited a fibrous consistency and a yellow color. Figure 10 shows the CDs at different scales. The one that provides the best resolution is 20 nm. The small black dots (spheres) scattered in the image are the CDs.

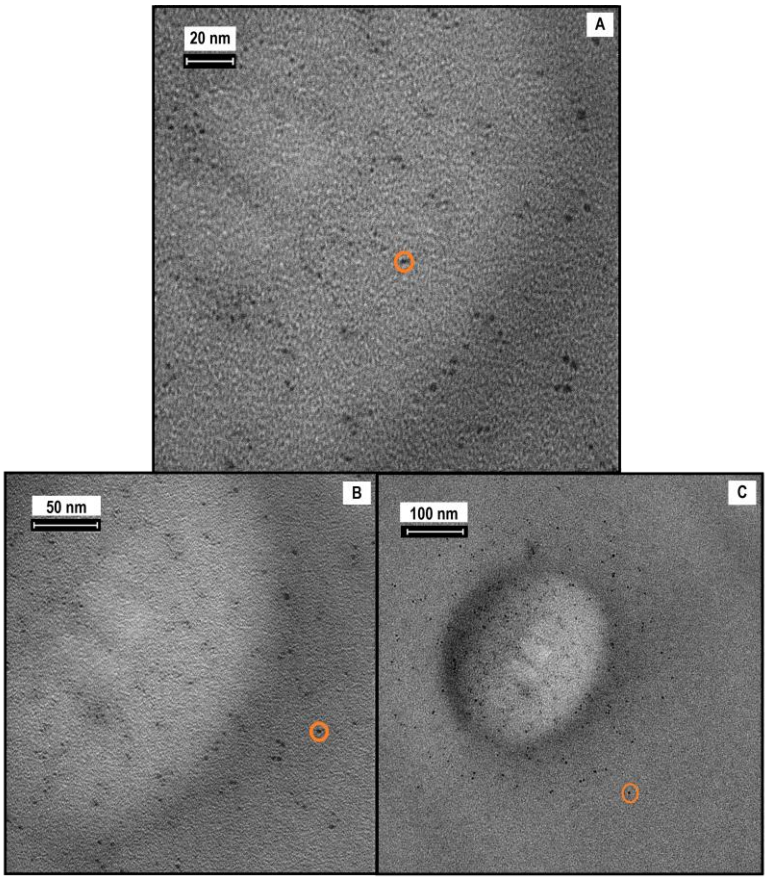

Figure 10. Results obtained from TEM in sample CD-180 with the presence of CDs.
Created by: Infante, Jordy, 2023.

After obtaining TEM images, spheres can be observed in the CD-180 sample. A total of 17 spheres were then labeled, and their pixel diameters were measured. Finally, the diameter of the spheres was calculated in nanometers using the value that 20 nm corresponds to 200 pixels. The calculations indicate that the obtained CDs have an average diameter of approximately 2.42 nm, with a range of 1.6 nm to 3.1 nm. Other CDs obtained from lignocellulosic residues have shown sizes in the range of 2-8 nm [20]; however, they underwent an additional aqueous extraction process in the hydrothermal synthesis. Despite that, the obtained size indicates that the spheres obtained are CDs because they have a size smaller than 10 nm. Fahmi *et al*. [50] also synthesized CDs from bamboo, but in this case, they used the leaves, and the particle size was 2 nm. In the results of Zhang *et al.* [20], the sugars that were carbonized in the hydrothermal synthesis were analyzed, and it was determined that they were the precursors for obtaining CDs. Therefore, by using bamboo lignocellulosic residues, it can be inferred that the chemical mechanism of action is similar, resulting in a similar size of the obtained CDs.

Additionally, it is worth noting that dialysis was not utilized in the purification process due to the lack of resources, unlike other synthesis methods [20,50], which employed dialysis smaller than 1000 kDa. This step can be optional, and its execution depends on the ease of extraction of the precursor molecules from the CDs, as well as on the degradation pathways proposed depending on the synthesis method. However, it often has a positive impact on the quality of the extract obtained, as mentioned in previous research [12]. In this report, the absence of this process could suggest that hydrothermal carbonization is a relatively simple process with room for improvement.

The temperature and synthesis time are crucial for evaluating the effectiveness of the proposed synthesis method, so further evaluation of the synthesized CDs under different conditions can be carried out.

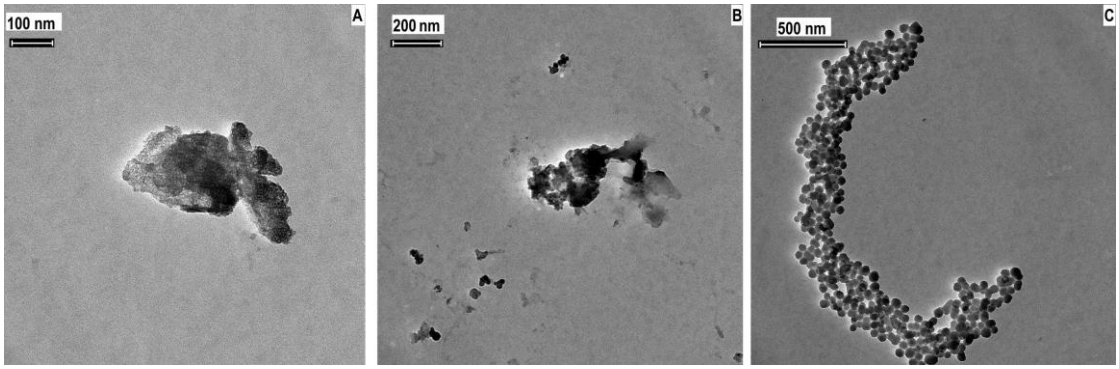

Figure 11. TEM images of B1 samples.
Created by: Infante, Jordy, 2023.

Regarding sample B1, a variable morphology can be observed in figure 11. Considering that this sample was a solid with multiple amorphous particles, it correlates with the observations in the TEM images, as they indicate the same, variable shapes in different parts of the analyzed sample but in all the images, there are clusters. It is worth noting that this sample is the lyophilized product of the obtained CDs, and there are no reports of TEM analysis on lyophilized CDs samples. Therefore, there is a knowledge gap regarding a standardized morphology of these lyophilized samples.

3.5 SEM analysis of CDs

SEM analysis (Scanning Electron Microscopy) was used to observe the surface morphology of the samples. The high-resolution images reveal details of the surface of the CDs, such as their shape, size, and structure. However, this assay is not informative due to the lack of desired sensitivity for the observation of CDs. In Figure 12, SEM images at 100 µ of the CD-180 and B1 samples can be observed. In both samples, a variable size, shape, and structure are observed, but the presence of CD nanoparticles is not as clearly visible as in the TEM assay.

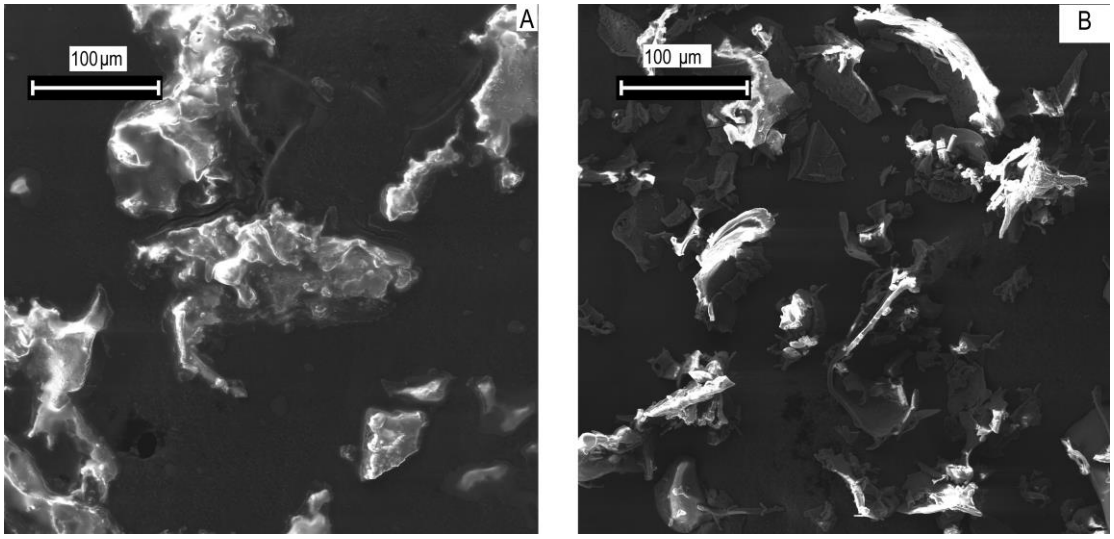

Figure 12. SEM images reported A) B1 samples B) CD-180 sample.
Created by: Infante, Jordy, 2023.

3.6 Energy Dispersive Spectroscopy of CDs

In the context of CDs synthesis, the EDS assay reported an elemental chemical profile of the B1 and CD-180 samples. However, the values obtained do not represent the true proportions because a carbon substrate was used in the assay, which caused the assay to not report the presence of carbon, thus altering the values of the elemental composition of the samples. Figure 13 shows the report of 7 elements for the B1 sample: oxygen, magnesium, silicon, phosphorus, sulfur, potassium, and calcium.

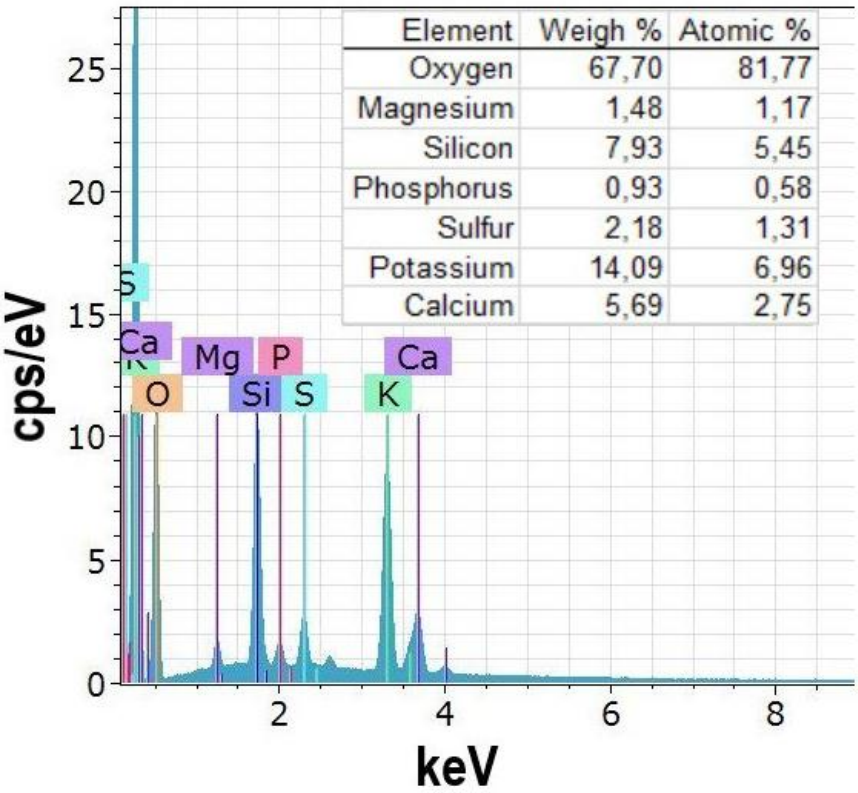

Figure 13. EDS reported of B1 sample.
Created by: Infante, Jordy, 2023.

The CD-180 sample (Figure 14) also reports the same elements except for phosphorus. Since no additional components were added to the CDs, the presence of phosphorus could be an impurity. Regarding the found values, they show similarities in proportions. Both samples have a high amount of oxygen and a low amount of sulfur, while the other elements show similar proportions. However, although these values do not indicate the actual elemental composition, it is evident that there is a wide variety of elemental components in both CD samples. Kumar et al. only obtained carbon and oxygen composition [67], while Pudza et al., obtained carbon, oxygen, and copper due to a doping process[29]. The CDs synthesized in this study were derived from residual bamboo biomass, which could have various elements in its composition, as reported.

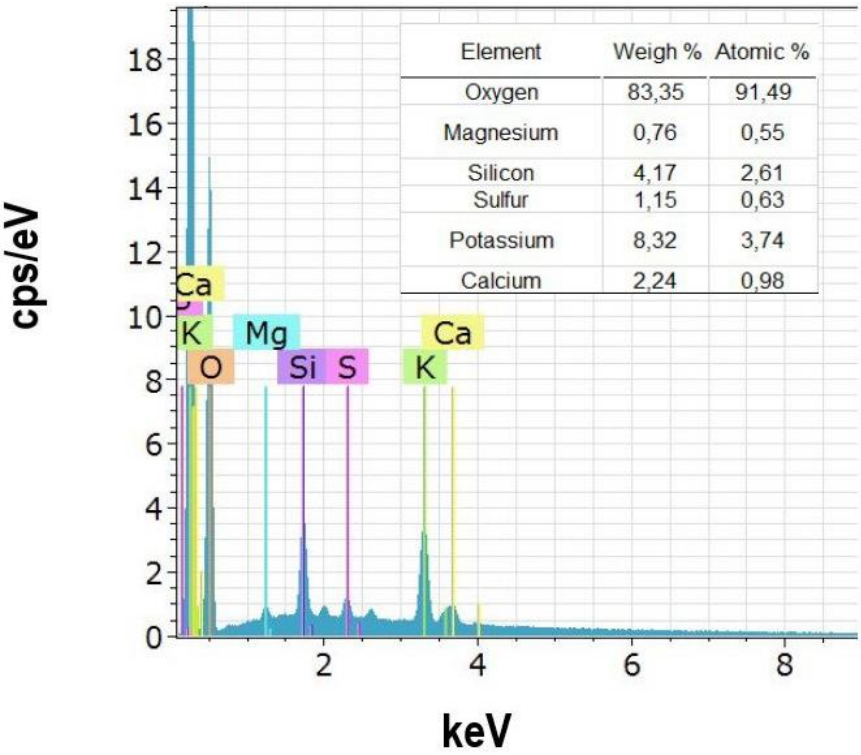

Figure 14. EDS reported of CD-180 sample.
Created by: Infante, Jordy, 2023.

3.7 Fourier transform infrared spectroscopy of CDs

FTIR spectroscopy provides valuable insights into the functional groups present in the CDs, allowing for a comprehensive understanding of their properties and potential applications. As shown in Figure 15, there are peaks associated with the stretching vibrations of hydroxyl (-OH) and carbonyl (COO-) groups, observed at wavelengths 3270 and 2936 cm^{-1}, respectively. The spectrum also exhibits other bands of interest. The band between 1330 and 1450 cm^{-1} indicates an alcohol (O-H), while the band between 1200 and 1300 cm^{-1} indicates an aromatic ester (C-O). The FT-IR graph illustrates the presence of unsaturated carbon and oxygen-rich functional groups, including hydroxyl, carboxyl, and carbonyl groups, on the surface of the carbon dots. These findings are consistent with the hydrothermal synthesis process of carbon dots. The identified functional groups contribute to the hydrophilic properties of the carbon dots, making them water-soluble.

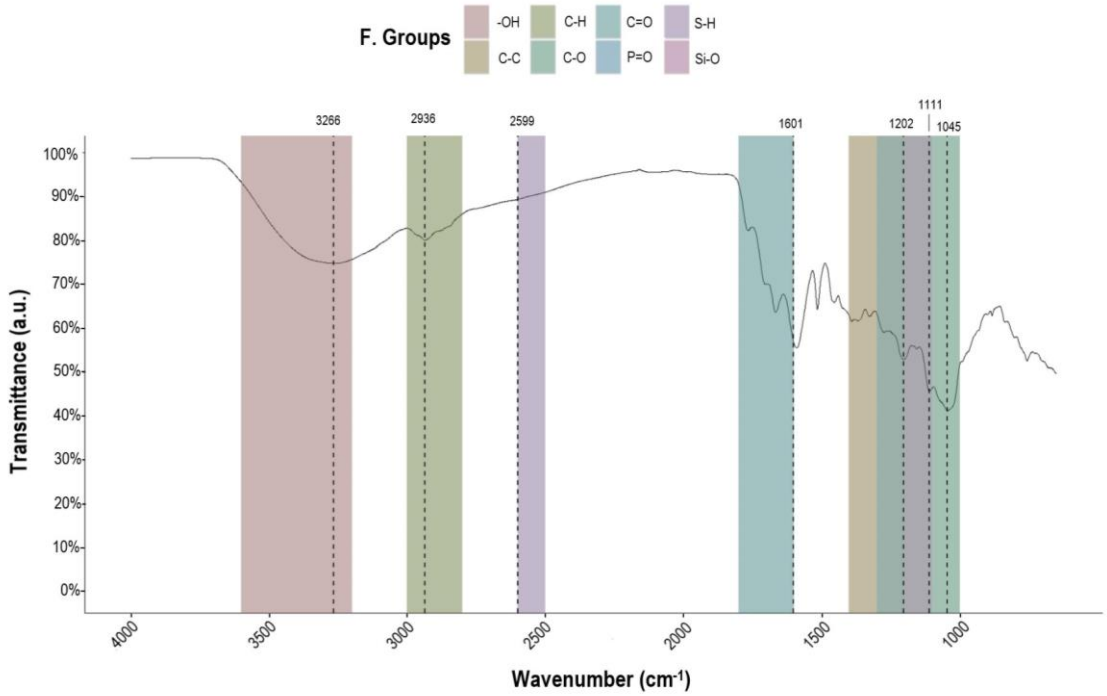

Figure 15. FTIR reported from B1 samples. 180°C – 300 min
Created by: Infante, Jordy, 2023.

Among other peaks of interest, the following were reported: 1516 cm^{-1} corresponding to C-O-C, 1094 cm^{-1} corresponding to C=C, 996 cm^{-1} potentially corresponding to C=O, and 706 cm^{-1} corresponding to C=C. The peak at 1516 cm^{-1} corresponding to C-O-C indicates the presence of ethers in the sample. This observation could be related to the biomass structure and the chemical composition of its components, such as cellulose and lignin [20]. The peak at 1094 cm^{-1}, which corresponds to C=C, suggests the presence of carbon-carbon double bonds. This finding can be attributed to the existence of aromatic organic compounds or conjugated polymers in the sample. The peak at 996 cm^{-1}, potentially corresponding to C=O, indicates the presence of carbonyl groups [51]. These functional groups are associated with compounds containing both carbon and oxygen, such as aldehydes and ketones. The peak at 706 cm^{-1}, also corresponding to C=C, once again suggests the presence of carbon-carbon double bonds [63]. This finding may be indicative of the presence of organic compounds with conjugated or unsaturated structures. The FT-IR graph illustrates the presence of unsaturated carbon and oxygen-rich functional groups, including hydroxyl, carboxyl, and carbonyl groups, on the surface of the carbon dots. These findings are consistent with the hydrothermal carbonization process of CDs [29]. The identified functional groups contribute to the hydrophilic properties of the carbon dots, making them water-soluble.

3.8 X-Ray Diffraction of CDs

XRD analysis can provide information about crystalline structure. However, due to the fact that CDs generally have an amorphous or nanocrystalline structures, XRD analysis may not reveal sharp diffraction peaks associated with a well-defined crystalline structure. For this reason, in Figures 16 and 17, different aspects of the patterns can be observed. Figure 16 corresponds to the lyophilized sample with well-defined signals, while Figure 17 shows the pattern of the CD-180 sample in liquid form, processed as a film on a glass slide. Its pattern appears broad and of low precision, as it presents background noise.

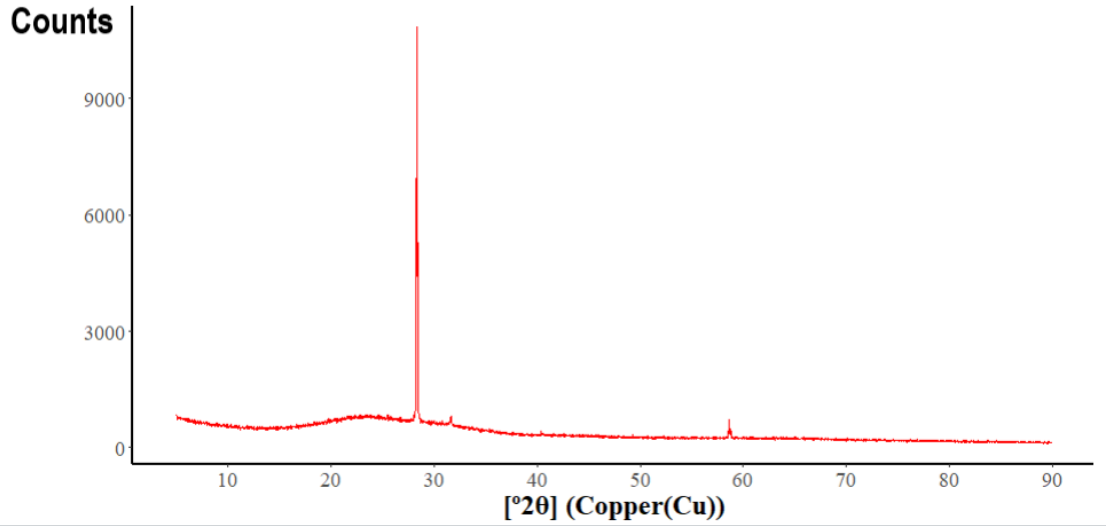

Figure 16. XRD from B1 sample.
Created by: Infante, Jordy, 2023.

This XRD report shows the presence of amorphous CDs, similar to several previous studies [16]. Figure 17 reveals the amorphous nature of the CDs, characterized by a broad diffraction peak between 15° to 25°, indicating a graphitic lattice spacing [66].

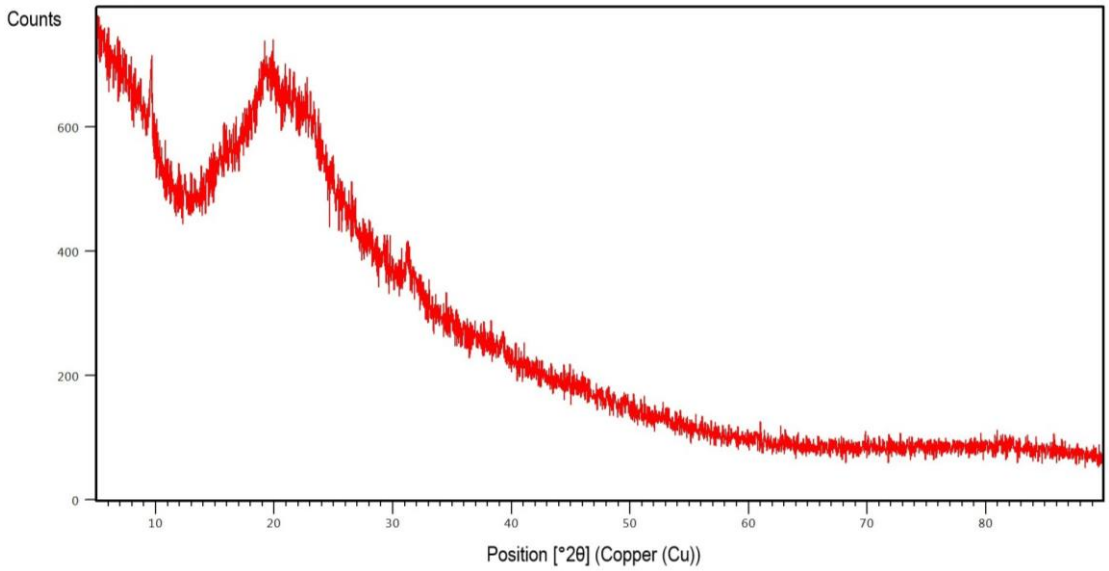

Figure 17. XRD from CD-180 sample.
Created by: Infante, Jordy, 2023.

This assay serves as a reference to confirm the functional groups obtained in the FTIR, and the data are consistent due to the presence of these functional groups in both assays. However, the FTIR provides more specific results.

3.9 Optimization through Response Surface Methodology

Figure 18 was made from the fluorescence data of the 12 experimental batches. The temperature ranged from 172 °C to 342 °C, and the residence time ranged from 257 min to 342 min. These points corresponded to the axial points proposed by the central composite design of type circumscribed. This method is suitable because it is an exploratory test that helps to evaluate a new experimental region or to determine the minimum or maximum points of optimization in the experiments being performed.

Several models were tested, among which a non-iterative equation was reported, taking fluorescence values as the reference response. In this model, the following quadratic equation was generated from a regression analysis:

$$F\ (a.u) = \ 4374 - 4.48T - 24.82t - 0.11\frac{T}{t} + 0.11T^2 + 0.07t^2$$

This equation has a goodness of fit, with an R^2 value of 0.8466 and an adjusted R^2 value of 0.7187. The parameters that the model response indicates that there no enough evidency to discart the nule hippothesis. Both R^2 value are satisfactory to indicate that

the model is expresion a good distribution of datas. In addition, this model reports a p-value = 0.01973, which indicates reliability in the experimental design. This model was also evaluated with the Akaike information criterion (AIC), which gave the best value of 139.87.

These values can be observed in table 4. This table also indicates, thanks to F_o, that the polynomial values of -4.48T and -24.82t carry significant weight in the reported formula, with temperature and time being the factors to consider. In addition, the p-value of the lack of fit indicates that there are no external factors influencing the process.

Table 4. ANOVA analysis of the reported quadratic model.

Source	**Sum Squares**	**df**	**Mean Squares**	**F_0**	**p-value**
FO(X1, X2)	79536	2	39768	9.4482	0.0139
TWI(X1, X2)	20592	1	20592	4.8924	0.0689
PQ(X1, X2)	39232	2	19616	4.6604	0.060062
Residual	25254	6	4209		
Lack of Fit	25047	3	8349	121.1487	0.001254
Pure error	207	3	69		
Stationary point	TEMP	169.80	TIME	283.01	
R^2= 0.8466	$R_{(ADJ)}^2$=	0.7187	AIC=	139.8766	

Created by: Infante, Jordy, 2023.

TWI() corresponds to the interactions between factors, PQ() refers to the pure quadratic terms, and FO() indicates the linear model [46]. These data correspond to the importance of time, which has a more significant effect on performance.

Figure 18 shows the response surface indicating the presence of stationary point, the model indicates that the stationary point is in the temperature 169°C and time 282 min. This stationary point corresponds to the presence of a minimum. The model indicates that the factors influence the response model in a very direct way, especially the temperature factor. This model is useful for a two-factor experiment but to increase the veracity of the model, further testing is recommended.

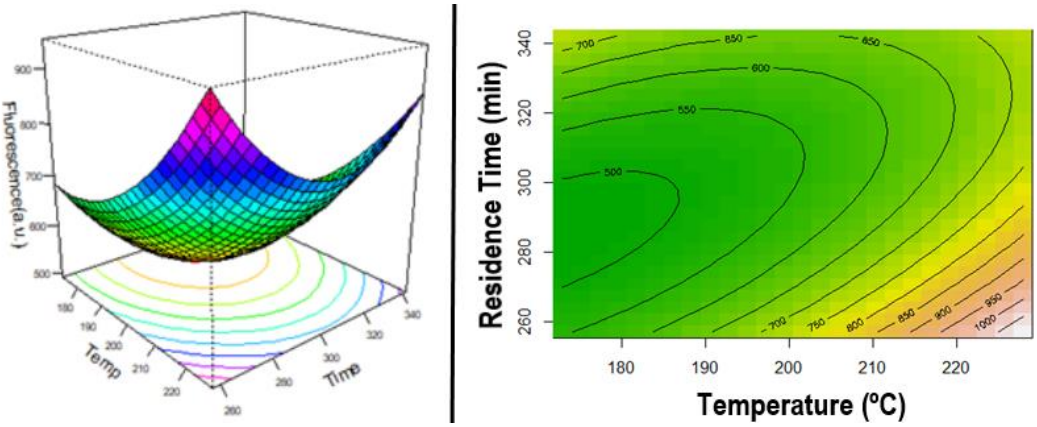

Figure 18. Response surface for the interaction between Time, Temperature and Fluorescence and contours.
Created by: Infante, Jordy, 2023.

In spite of having indicators that prove that the model serves to analyze the behavior of the variables, the model obtained has several improvements to consider. A minimum is found in it; however optimal values are sought in order to get closer to a desired experimental region. Therefore, in order for the model to become optimal, a new experimental region must be chosen. The CD-2 synthesis conditions, 200°C and 270 min, are candidates to be the new center of the new experimental region. This new experimental design should also take into account the minimum point reported in this design, 169.80°C and 283.01 min. An experimental region containing these points would indicate a more complete experimental behavior, which can help to better understand how the variables vary with each other and better optimize the process.

CONCLUSIONS AND FUTURE PERSPECTIVES

This study utilized bamboo woody residues (BWR) as a precursor due to their polysaccharide-rich composition containing cellulose, lignin, hemicellulose, and holocellulose. These compounds offer valuable properties like stability, hardness, and abundance. The specific polysaccharides were identified through high-performance liquid chromatography (HPLC) equipped with a SP-G guard column and a SP-0810 analytical column and thermogravimetric analysis (TGA) to quantify carbon content, enhancing the understanding of hydrothermal carbonization. The hydrothermal synthesis process effectively extracted polysaccharides for Carbon Dots (CDs) formation. Temperature and time were critical factors, with temperature notably influencing optical qualities. Optimal conditions were determined at CD-2 with 220°C-270 minutes, resulting in the highest CD concentration. The study underscored time's role in enhancing optical qualities, like absorbance, so the synthesis method is reproducible to increase the chemical and physical properties.

The synthesized CDs displayed potential as biosensors due to distinct fluorescence properties. Although further CD characterization is required, the study confirms the promise of hydrothermal synthesis from bamboo woody residues in producing CDs with favorable fluorescence properties. This approach aligns with green synthesis principles, employing renewable biomass and contributing to eco-friendly production processes. Focusing on green synthesis methods is vital, aiming for reduced environmental impact and sustainable CDs production. In this report six principles of green chemistry were developed, such as safe synthesis process (3), use of safer chemicals (4), use of safe solvents (5), energy saving (6), use of renewable raw materials (7), and use of safe chemical processes (12). There are others principles that can be developed after this project, such as reduce derivatives (8) and prevent waste (1). The implementation of physical and chemical analysis could help to design another synthesis method with more green principles.

Future prospects involve toxicity assays for biomedical applications, including bioimaging and molecular transport. Detection assays will explore CDs applicability in biosensors, utilizing their unique attributes for selective substance detection. Adsorption assays will assess CDs potential in environmental contexts, such as water or air

contaminant removal. Conductivity assays could unveil CDs' role as semiconductors in electronic devices, expanding nanoelectronics possibilities.

CDs structure enhancement through element doping and heterojunction formation could unlock new applications. Iterative experimental design refinement will optimize synthesis, enhancing CDs efficiency and revealing untapped potential.

REFERENCES

1. National Research Council. A research strategy for environmental, health, and safety aspects of engineered nanomaterials. 2012. doi:10.17226/13347
2. Marrapese ME. Part 8 Regulation of Bio -nanotechnology.
3. Edvinsson T. Optical quantum confinement and photocatalytic properties in two-, one- and zerodimensional nanostructures. R Soc Open Sci. 2018;5. doi:10.1098/rsos.180387
4. Arias Velasco V, Caicedo Chacón WD, Carvajal Soto AM, Ayala Valencia G, Granada Echeverri JC, Agudelo Henao AC. Carbon Quantum Dots Based on Carbohydrates as Nano Sensors for Food Quality and Safety. Starch/Staerke. 2021;73. doi:10.1002/star.202100044
5. Zhi B, Yao XX, Cui Y, Orr G, Haynes CL. Synthesis, applications and potential photoluminescence mechanism of spectrally tunable carbon dots. Nanoscale. 2019;11: 20411–20428. doi:10.1039/c9nr05028k
6. Scaria J, Karim A V., Divyapriya G, Nidheesh P V., Suresh Kumar M. Carbon-supported semiconductor nanoparticles as effective photocatalysts for water and wastewater treatment. Nano-Materials as Photocatalysts for Degradation of Environmental Pollutants: Challenges and Possibilities. Elsevier Inc.; 2019. doi:10.1016/B978-0-12-818598-8.00013-4
7. Jani M, Arcos-Pareja JA, Ni M. Engineered Zero-Dimensional Fullerene/Carbon Dots-Polymer Based Nanocomposite Membranes for Wastewater Treatment. Molecules. 2020;25: 1–28. doi:10.3390/molecules25214934
8. Dinç S, Kara M, Yavuz E. Synthesis of carbon dots from biomass resources. Carbon Dots in Agricultural Systems: Strategies to Enhance Plant Productivity. 2022. doi:10.1016/B978-0-323-90260-1.00001-2
9. Cui L, Ren X, Sun M, Liu H, Xia L. Carbon dots: Synthesis, properties and applications. Nanomaterials. 2021;11. doi:10.3390/nano11123419
10. Koutsogiannis P, Thomou E, Stamatis H, Gournis D, Rudolf P. Advances in fluorescent carbon dots for biomedical applications. Adv Phys X. 2020;5. doi:10.1080/23746149.2020.1758592
11. El-Shabasy RM, Elsadek MF, Ahmed BM, Farahat MF, Mosleh KM, Taher MM. Recent developments in carbon quantum dots: Properties, fabrication techniques, and bio-applications. Processes. 2021;9: 1–24. doi:10.3390/pr9020388
12. Chahal S, Macairan JR, Yousefi N, Tufenkji N, Naccache R. Green synthesis of carbon dots and their applications. RSC Adv. 2021;11: 25354–25363. doi:10.1039/d1ra04718c
13. Jing HH, Bardakci F, Akgöl S, Kusat K, Adnan M, Alam MJ, et al. Green Carbon Dots: Synthesis, Characterization, Properties and Biomedical Applications. J Funct Biomater. 2023;14. doi:10.3390/jfb14010027
14. Ghosh D, Sarkar K, Devi P, Kim KH, Kumar P. Current and future perspectives of carbon and graphene quantum dots: From synthesis to strategy for building optoelectronic and energy devices. Renew Sustain Energy Rev. 2021;135: 110391. doi:10.1016/j.rser.2020.110391
15. Zanella R(UNA de M de CA y DT. Metodologías para la síntesis de nanopartículas: controlando forma y tamaño. Mundo Nano. 2012;5: 69–81. Available: https://www.scielo.org.mx/pdf/mn/v5n1/2448-5691-mn-5-01-69.pdf
16. Yuan M, Zhong R, Gao H, Li W, Yun X, Liu J, et al. One-step, green, and economic synthesis of water-soluble photoluminescent carbon dots by hydrothermal treatment of wheat straw, and their bio-applications in labeling, imaging, and sensing. Appl Surf Sci. 2015;355: 1136–1144.

doi:10.1016/j.apsusc.2015.07.095
17. Warner JC, Cannon AS, Dye KM. Green chemistry. Environ Impact Assess Rev. 2004;24: 775–799. doi:10.1016/j.eiar.2004.06.006
18. Papaioannou N, Titirici MM, Sapelkin A. Investigating the Effect of Reaction Time on Carbon Dot Formation, Structure, and Optical Properties. ACS Omega. 2019;4: 21658–21665. doi:10.1021/acsomega.9b01798
19. Ng HKM, Lim GK, Leo CP. Comparison between hydrothermal and microwave-assisted synthesis of carbon dots from biowaste and chemical for heavy metal detection: A review. Microchem J. 2021;165: 106116. doi:10.1016/j.microc.2021.106116
20. Zhang L, Lyu S, Zhang Q, Chmely SC, Wu Y, Melcher C, et al. Recycling hot-water extractions of lignocellulosic biomass in bio-refinery for synthesis of carbon nanoparticles with amplified luminescence and its application in temperature sensing. Ind Crops Prod. 2020;145: 112066. doi:10.1016/j.indcrop.2019.112066
21. Magagula LP, Masemola CM, Ballim MA, Tetana ZN, Moloto N, Linganiso EC. Lignocellulosic Biomass Waste-Derived Cellulose Nanocrystals and Carbon Nanomaterials: A Review. Int J Mol Sci. 2022;23. doi:10.3390/ijms23084310
22. Yoganandham ST, Sathyamoorthy G, Renuka RR. Emerging extraction techniques: Hydrothermal processing. Sustainable Seaweed Technologies: Cultivation, Biorefinery, and Applications. Elsevier Inc.; 2020. doi:10.1016/B978-0-12-817943-7.00007-X
23. Thangaraj B, Solomon PR, Ranganathan S. Synthesis of Carbon Quantum Dots with Special Reference to Biomass as a Source - A Review. Curr Pharm Des. 2019;25: 1455–1476. doi:10.2174/1381612825666190618154518
24. García SM. Ecuador: Estrategia Nacional del Bambú. 2019. Available: https://bambuecuador.files.wordpress.com/2019/03/estrategia-nacional-bambc3ba-2018-2022-versic3b3n-resumida.pdf
25. Hoekman SK, Broch A, Robbins C. Hydrothermal carbonization (HTC) of lignocellulosic biomass. Energy and Fuels. 2011;25: 1802–1810. doi:10.1021/ef101745n
26. Xiao LP, Shi ZJ, Xu F, Sun RC. Hydrothermal carbonization of lignocellulosic biomass. Bioresour Technol. 2012;118: 619–623. doi:10.1016/j.biortech.2012.05.060
27. Bai J, Yuan G, Chen X, Zhang L, Zhu Y, Wang X, et al. Simple Strategy for Scalable Preparation Carbon Dots: RTP, Time-Dependent Fluorescence, and NIR Behaviors. Adv Sci. 2022;9: 1–9. doi:10.1002/advs.202104278
28. Pudza MY, Abidin ZZ, Rashid SA, Yasin FM, Noor ASM, Issa MA. Sustainable synthesis processes for carbon dots through response surface methodology and artificial neural network. Processes. 2019;7. doi:10.3390/pr7100704
29. Pudza MY, Abidin ZZ, Rashid SA, Yasin FM, Noor ASM, Issa MA. Eco-friendly sustainable fluorescent carbon dots for the adsorption of heavy metal ions in aqueous environment. Nanomaterials. 2020;10. doi:10.3390/nano10020315
30. Pourmahdi N, Sarrafi AHM, Larki A. Carbon Dots Green Synthesis for Ultra-Trace Determination of Ceftriaxone Using Response Surface Methodology. J Fluoresc. 2019;29: 887–897. doi:10.1007/s10895-019-02400-5
31. Shi X, Wei W, Fu Z, Gao W, Zhang C, Zhao Q, et al. Review on carbon dots in food safety applications. Talanta. 2019;194: 809–821. doi:10.1016/j.talanta.2018.11.005
32. Zhang J, Yin H, Shen Y, Bai M, Wan J. Preparation of Carbon Quantum Dots for Fluorescence Detection of Environmental Pollutants. J Nanosci Nanotechnol. 2019;19: 5522–5528.

doi:10.1166/jnn.2019.16928

33. Fatahi Z, Esfandiari N, Ehtesabi H, Bagheri Z, Tavana H, Ranjbar Z, et al. Physicochemical and cytotoxicity analysis of green synthesis carbon dots for cell imaging. EXCLI J. 2019;18: 454–466. doi:10.17179/excli2019-1465
34. Hashemi F, Heidari F, Mohajeri N, Mahmoodzadeh F, Zarghami N. Fluorescence Intensity Enhancement of Green Carbon Dots: Synthesis, Characterization and Cell Imaging. Photochem Photobiol. 2020;96: 1032–1040. doi:10.1111/php.13261
35. Ehtesabi H, Hallaji Z, Najafi Nobar S, Bagheri Z. Carbon dots with pH-responsive fluorescence: a review on synthesis and cell biological applications. Microchim Acta. 2020;187. doi:10.1007/s00604-019-4091-4
36. Feng H, Qian Z. Functional Carbon Quantum Dots: A Versatile Platform for Chemosensing and Biosensing. Chem Rec. 2018;18: 491–505. doi:10.1002/tcr.201700055
37. Chen J, Liu J, Dai J, Lin B, Gao C, Wang C. Reservoir Adaptability Evaluation and Application Technology of Carbon Quantum Dot Fluorescent Tracer. Eng. 2023;4: 703–718. doi:10.3390/eng4010042
38. Han Y, Yang W, Luo X, He X, Zhao H, Tang W, et al. Carbon dots based ratiometric fluorescent sensing platform for food safety. Crit Rev Food Sci Nutr. 2022;62: 244–260. doi:10.1080/10408398.2020.1814197
39. Hames B, Ruiz R, Scarlata C, Sluiter A, Sluiter J, Templeton D. Preparation of Samples for Compositional Analysis: Laboratory Analytical Procedure (LAP); Issue Date 08/08/2008. 2008.
40. Sluiter A, Hames B, Hyman D, Payne C, Ruiz R, Scarlata C, et al. Determination of total solids in biomass and total dissolved solids in liquid process samples. Natl Renew Energy Lab. 2008; 3–5.
41. Sluiter A, Hames B, Hyman D, Payne C, Ruiz R, Scarlata C, et al. Determination of Ash in Biomass. Lab Anal Proced. 2008;36: 302–305.
42. Buchanan M, Tappi, This S. Solvent extractives of wood and pulp. Nanofibers - Prod Prop Funct Appl. 2007; 1–6. doi:10.5772/916
43. Tappi, (Organization) TA of the P and PI. One percent sodium hydroxide solubility of wood and pulp. Quality. 2011; 1–7.
44. Álvarez A, Cachero S, González-Sánchez C, Montejo-Bernardo J, Pizarro C, Bueno JL. Novel method for holocellulose analysis of non-woody biomass wastes. Carbohydr Polym. 2018;189: 250–256. doi:10.1016/j.carbpol.2018.02.043
45. Tappi, (Organization) TA of the P and PI. Lignin in Wood and Pulp. T222 Om-02. 2011; 1–7.
46. Lenth R V. Response-surface methods in R, using RSM. J Stat Softw. 2009;32: 1–17. doi:10.18637/jss.v032.i07
47. Mäntele W, Deniz E. UV–VIS absorption spectroscopy: Lambert-Beer reloaded. Spectrochim Acta - Part A Mol Biomol Spectrosc. 2017;173: 965–968. doi:10.1016/j.saa.2016.09.037
48. Gárate AERP, Felissia FE, Area MC, Suirezs T, Vallejos ME. Physical, Chemical and Morphological Characteristics of Bamboo Species Guadua Trinii and Guadua Angustifolia and Their Potential To Produce High-Value Products. Cellul Chem Technol. 2021;55: 951–959. doi:10.35812/cellulosechemtechnol.2021.55.81
49. Marafon AC, Amaral AFC, De Lemos EEP. Characterization of bamboo species and other biomasses with potential for thermal energy generation. Pesqui Agropecu Trop. 2019;49: 1–5. doi:10.1590/1983-40632019v4955282
50. Fahmi MZ, Haris A, Permana AJ, Nor Wibowo DL, Purwanto B, Nikmah YL, et al. Bamboo leaf-based carbon dots for efficient tumor imaging and therapy. RSC Adv. 2018;8: 38376–38383.

doi:10.1039/c8ra07944g

51. Liu Z, Jin W, Wang F, Li T, Nie J, Xiao W, et al. Ratiometric fluorescent sensing of Pb2+ and Hg2+ with two types of carbon dot nanohybrids synthesized from the same biomass. Sensors Actuators, B Chem. 2019;296: 126698. doi:10.1016/j.snb.2019.126698
52. Yang X, Wang D, Luo N, Feng M, Peng X, Liao X. Green synthesis of fluorescent N,S-carbon dots from bamboo leaf and the interaction with nitrophenol compounds. Spectrochim Acta - Part A Mol Biomol Spectrosc. 2020;239: 118462. doi:10.1016/j.saa.2020.118462
53. César MF, Hilario F, Callupe N, Cruz L, Caller JL, Gonzales HE. Caracterización Química Y Física Del Bambú. Av en Ciencias e Ing. 2019;10: 1–13. Available: http://www.executivebs.org/publishing.cl/%0Ahttps://www.executivebs.org/publishing.cl/aci/2019/Vol10/Nro4/1-ACI1336-19-full.pdf
54. Wei H, Yingting Y, Jingjing G, Wenshi Y, Junhong T. Lignocellulosic Biomass Valorization: Production of Ethanol. Encyclopedia of Sustainable Technologies. Elsevier; 2017. doi:10.1016/B978-0-12-409548-9.10239-8
55. Madan A, Pare A. Drying and Rehydration Behaviour of Bamboo (Bambusa bambos) Shoots during Convective Tray Drying. Online) J AgriSearch. 2014;1: 127–134.
56. Liu Z, Zhang T, Zhang J, Xiang H, Yang X, Hu W, et al. Ash fusion characteristics of bamboo, wood and coal. Energy. 2018;161: 517–522. doi:10.1016/j.energy.2018.07.131
57. Li W, Wang S, Li Y, Ma C, Huang Z, Wang C, et al. One-step hydrothermal synthesis of fluorescent nanocrystalline cellulose/carbon dot hydrogels. Carbohydr Polym. 2017;175: 7–17. doi:10.1016/j.carbpol.2017.07.062
58. Li Y, Bi J, Liu S, Wang H, Yu C, Li D, et al. Presence and formation of fluorescence carbon dots in a grilled hamburger. Food Funct. 2017;8: 2558–2565. doi:10.1039/c7fo00675f
59. Wang J, Chu Y, Qiu F, Li X, Wu H, Pan J, et al. WITHDRAWN: One-pot simple green synthesis of water-soluble cleaner fluorescent carbon dots from cellulose and its sensitive detection of iron ion. J Clean Prod. 2017. doi:10.1016/j.jclepro.2017.07.187
60. Perumal S, Atchudan R, Thirukumaran P, Yoon DH, Lee YR, Cheong IW. Simultaneous removal of heavy metal ions using carbon dots-doped hydrogel particles. Chemosphere. 2022;286: 131760. doi:10.1016/j.chemosphere.2021.131760
61. Boruah A, Saikia M, Das T, Goswamee RL, Saikia BK. Blue-emitting fluorescent carbon quantum dots from waste biomass sources and their application in fluoride ion detection in water. J Photochem Photobiol B Biol. 2020;209: 111940. doi:10.1016/j.jphotobiol.2020.111940
62. Hasan MR, Saha N, Quaid T, Toufiq Reza M. Formation of carbon quantum dots via hydrothermal carbonization: Investigate the effect of precursors. Energies. 2021;14: 1–10. doi:10.3390/en14040986
63. Senthamizhan A, Fragouli D, Balusamy B, Patil B, Palei M, Sabella S, et al. Hydrochromic carbon dots as smart sensors for water sensing in organic solvents. Nanoscale Adv. 2019;1: 4258–4267. doi:10.1039/c9na00493a
64. An J, Chen M, Hu N, Hu Y, Chen R, Lyu Y, et al. Carbon dots-based dual-emission ratiometric fluorescence sensor for dopamine detection. Spectrochim Acta - Part A Mol Biomol Spectrosc. 2020;243: 118804. doi:10.1016/j.saa.2020.118804
65. Lu W, Qin X, Liu S, Chang G, Zhang Y, Luo Y, et al. Economical, green synthesis of fluorescent carbon nanoparticles and their use as probes for sensitive and selective detection of mercury(II) ions. Anal Chem. 2012;84: 5351–5357. doi:10.1021/ac3007939
66. Wang M, Shi R, Gao M, Zhang K, Deng L, Fu Q, et al. Sensitivity fluorescent switching sensor for Cr

(VI) and ascorbic acid detection based on orange peels-derived carbon dots modified with EDTA. Food Chem. 2020;318: 126506. doi:10.1016/j.foodchem.2020.126506

67. Kumar VB, Kumar R, Gedanken A, Shefi O. Fluorescent metal-doped carbon dots for neuronal manipulations. Ultrason Sonochem. 2019;52: 205–213. doi:10.1016/j.ultsonch.2018.11.017

ANEXES

3.10 Response of model in Rstudio

```
             Estimate  Std. Error t value Pr(>|t|)
(Intercept) 4374.133987 5160.169430  0.8477  0.42913
x1            -4.483203   31.317025 -0.1432  0.89085
x2           -24.829189   20.148068 -1.2323  0.26392
x1:x2         -0.119583    0.054064 -2.2119  0.06897 .
x1^2           0.112859    0.066806  1.6893  0.14211
x2^2           0.079739    0.028337  2.8140  0.03060 *
---
Signif. codes:  0 ‘***’ 0.001 ‘**’ 0.01 ‘*’ 0.05 ‘.’ 0.1 ‘ ’ 1

Multiple R-squared:  0.8466,    Adjusted R-squared:  0.7187
F-statistic: 6.622 on 5 and 6 DF,  p-value: 0.01973
```

```
Multiple R-squared:  0.8458,    Adjusted R-squared:  0.7172
F-statistic: 6.581 on 5 and 6 DF,  p-value: 0.02003

Analysis of Variance Table

Response: y1
            Df Sum Sq Mean Sq  F value   Pr(>F)
FO(x1, x2)   2  79420   39710   9.3859 0.014210
TWI(x1, x2)  1  20722   20722   4.8978 0.068850
PQ(x1, x2)   2  39064   19532   4.6166 0.061106
Residuals    6  25385    4231
Lack of fit  3  25168    8389 116.0392 0.001337
Pure error   3    217      72

Stationary point of response surface:
      x1       x2
169.6103 282.7739

Stationary point in original units:
    Temp     Time
169.6103 282.7739
```

3.11 Response of model adjusted in Rstudio

```
             Estimate  Std. Error t value Pr(>|t|)
(Intercept)  1.1549e+04  5.0060e+03  2.3071  0.05442 .
x1          -4.0358e+01  3.3418e+01 -1.2077  0.26639
x2          -4.8746e+01  2.1207e+01 -2.2986  0.05511 .
x1^2         1.1286e-01  8.3335e-02  1.3543  0.21774
x2^2         7.9739e-02  3.5348e-02  2.2558  0.05869 .
---
Signif. codes:  0 ‘***’ 0.001 ‘**’ 0.01 ‘*’ 0.05 ‘.’ 0.1 ‘ ’ 1

Multiple R-squared:  0.7215,    Adjusted R-squared:  0.5623
F-statistic: 4.533 on 4 and 7 DF,  p-value: 0.04019
```

```
Multiple R-squared:  0.7199,    Adjusted R-squared:  0.5598
F-statistic: 4.497 on 4 and 7 DF,  p-value: 0.04095

Analysis of Variance Table

Response: y1
            Df Sum Sq Mean Sq  F value    Pr(>F)
FO(x1, x2)   2  79420   39710   6.0289 0.0300328
PQ(x1, x2)   2  39064   19532   2.9654 0.1167242
Residuals    7  46107    6587
Lack of fit  4  45890   11472 158.6833 0.0008043
Pure error   3    217      72

Stationary point of response surface:
      x1       x2
178.7818 305.6842

Stationary point in original units:
    Temp     Time
178.7818 305.6842
```

3.12 Tabla de cálculo de tamaño de diámetro de CDs

Tabla 1-A. Cálculo de tamaño de diámetro de CDs. Po: pixel inicial; Pf: pixel final; Pt: píxeles totales.

N	Po	Pf	Pt	nm
A	846	865	19	1,90
B	869	890	21	2,10
C	1100	1118	18	1,80
D	1346	1367	21	2,10
E	1913	1934	21	2,10
F	1761	1790	29	2,90
G	1813	1844	31	3,10
H	1216	1247	31	3,10
I	1800	1828	28	2,80
J	1837	1868	31	3,10
K	1419	1439	20	2,00
L	1811	1842	31	3,10
M	1893	1926	33	3,30
N	599	618	19	1,90
Ñ	952	970	18	1,80
O	597	622	25	2,50
P	968	984	16	1,60
		TAMAÑO PROMEDIO:		2,42

Created by: Infante, Jordy, 2023

3.13 Tabla de resultados de FTIR

Table 2. FTIR ESSAY

Wavelength (cm^{-1})	Intensity (a.u.)	Associated component description
3270	74.80	-OH
2936	80.04	COO-
2125	95.58	C-H
1667	63.70	C-O-C
1590	55.54	C=C
1516	64.36	C–O–C
1094	-	C=C
996	-	C=O
706	-	C=C

Created by: Infante, Jordy, 2023

3.14 Diagrama de flujo del presente proyecto